Golder Associates Inc.

1951 Old Cuthbert Road, Suite 301
Cherry Hill, NJ 08034
Tel: (856) 616-8166
Fax: (856) 616-1874

REPORT ON

INFLUENCE OF BIOATTENUATION ON VAPOR INTRUSION INTO BUILDINGS – MODEL SIMULATIONS USING SEMI-ANALYTICAL ONE-DIMENSIONAL MODEL

Submitted to:

New Jersey Department of Environmental Protection
Division of Science, Research, and Technology
P.O. Box 409
Trenton, NJ 08625

Attention: Dr. Paul F. Sanders

DISTRIBUTION:

5 Copies:	NJDEP, Trenton, NJ
1 Copy:	Dr. Paul C. Johnson, ASU
1 Copy:	Golder Cherry Hill, NJ, USA,
1 Copy:	Golder Amherst, MA, USA
2 Copies:	Golder Associates Ltd., Burnaby, BC, Canada

September 2006 023-6124-001

SUMMARY

This report, prepared by Golder Associates Inc. (Golder Associates) for the New Jersey Department of Environmental Protection (NJDEP), describes the results of our research study of the influence of bioattenuation on vapor intrusion through model simulations using a semi-analytical one-dimensional fate and transport model. This study has been completed as part of a research study titled "*Investigation of Indoor Air Quality in Structures Located Above VOC-Contaminated Groundwater*", which is being conducted by Golder Associates for the New Jersey Department of Environmental Protection (NJDEP). The purpose of this research program is to evaluate soil vapor intrusion into buildings through field measurements, comparisons of measured attenuation factors to existing guidance for vapor intrusion, and mathematical modeling of vapor intrusion.

The migration of chemical vapors from subsurface sources into buildings is an exposure pathway that is increasingly being assessed at petroleum hydrocarbon (e.g. BTEX) contaminated sites. Since many hydrocarbon compounds are readily biodegraded under aerobic conditions, there is significant interest from regulators, owners and other stakeholders in approaches and predictive models that incorporate aerobic bioattenuation into the assessment of the vapor intrusion pathway. Several regulatory agencies have developed groundwater screening levels that are derived using generic attenuation factors that incorporate a 10X reduction factor for bioattenuation (New Jersey Department of Environment (NJDEP), Massachusetts Department of Environmental Protection (MADEP), and San Francisco Regional Water Quality Control Board's (RWQCB)). While there is limited empirical data that indicates bioattenuation at some sites results in lower attenuation factors for BTEX chemicals than those observed for non-degrading chemicals, only limited rationale is provided in the above guidance for the empirical reduction factor chosen (i.e., 10X).

The objectives of this modeling study are to evaluate factors affecting hydrocarbon vapor biodegradation, and through model simulations and comparisons to field data, facilitate the development of regulatory guidance and reduction factors for aerobically degradable hydrocarbon compounds. The model used for this study is a new one-dimensional model ("J&E-BIO model") for vapor intrusion that is based on the Johnson and Ettinger (1991) model framework, but that includes oxygen-limited first-order or zero-order biodegradation through a semi-analytical numerical solution using the SOLVER routine in Excel. First- or zero-order biodegradation is limited to a single dominant soil layer (Johnson et al., 1998). The model simulates transport through up to eight soil layers and thus has the capability of simulating transport through a variably saturated soil profile (e.g., capillary transition zone).

The approach used for the modeling study was to first bench-mark the J&E-BIO model against the 3-D numerical model results by Abreu and Johnson (2006), which were for a homogeneous soil profile. The J&E-BIO model was then used to evaluate several different scenarios relative to the base case simulations to provide insight on the influence that different factors have on bioattenuation. Since the J&E-BIO model makes simplifying assumptions for oxygen transport and biodegradation, the model predictions are approximate. The J&E-BIO model, nevertheless, is a useful tool for rapid evaluation of bioattenuation.

The J&E-BIO model predictions for a homogeneous soil profile indicate that the vapor attenuation factor is dependent primarily on the vapor source strength and to a lesser extent, the separation distance between the source and building foundation. For model predictions without oxygen-limited biodegradation, the J&E-BIO model over-predicted bioattenuation compared to the Abreu and Johnson 3-D model for high source strength (i.e., concentrations representative of a gasoline source). The model simulations highlight that a model that does not include consideration of oxygen limitations may under predict vapor intrusion when there are high source hydrocarbon concentrations.

Other important findings of the modeling study were that higher soil moisture, as found within the capillary fringe, significantly reduces volatilisation flux of hydrocarbons. As a consequence, the model simulations suggest oxygen limitations below buildings above dissolved hydrocarbon sources would be rare, except when contamination was very shallow. The model simulations suggest that the influence of wind on oxygenation below buildings will typically be relatively minor. Barometric pressure changes may result in increased transport of hydrocarbon vapors relative to mass flux through diffusion alone; however, the same process should also result in enhanced oxygen transport to below the building. The modeling suggests competent low permeability or diffusivity surface barriers may significantly reduce oxygenation below buildings.

The implications of the modeling study for regulatory guidance are that a 10X reduction factor to account for bioattenuation would be justified for many sites. Exceptions would be sites with gasoline contamination, residual non-aqueous phase liquid (NAPL) present above the water table, with moderate to shallow contamination (i.e., less than about 5 m separation distance). For sites with only dissolved petroleum hydrocarbon contamination, there is likely to be sufficient oxygenation below building foundations to result in significant bioattenuation.

A regulatory framework using soil vapor measurements is recommended for evaluation of bioattenuation. Soil vapor is preferable over groundwater since there is uncertainty in delineation of NAPL zones and predictive models for transport within the capillary fringe. In addition, since dissolved plumes tend to be relatively short, as a practical consequence, there may be limited ability to screen out sites based on groundwater data alone. Empirical reduction factors for bioattenuation are proposed for generic soil vapor attenuation factors based on modeling results presented in this study and those given in Abreu and Johnson (2006). It is important that bioattenuation reduction factors be applied in the context of a protocol for soil vapor characterization and lines-of-evidence evaluation of biodegradation, to confirm biodegradation is occurring and the absence of precluding factors such as a significant capping effect. Soil vapor concentrations measured near to the contamination source should be used for assessment of bioattenuation.

ACKNOWLEDGEMENTS

The helpful review comments of Dr. Paul Sanders and guidance provided throughout this research project are gratefully acknowledged.

TABLE OF CONTENTS

LIST OF TABLES

LIST OF FIGURES

1.0 INTRODUCTION

The migration of chemical vapors from subsurface sources into buildings is an exposure pathway that is increasingly being assessed at petroleum hydrocarbon (e.g. BTEX) contaminated sites. Since many hydrocarbon compounds are readily biodegraded under aerobic conditions, there is significant interest from regulators, owners and other stakeholders in approaches and predictive models that incorporate aerobic bioattenuation into the assessment of the vapor intrusion pathway. Helpfully, there are an increasing number of studies that provide data on the vapor attenuation factor ("alpha"), which is the ratio between indoor vapor and soil vapor concentrations. This data indicates that vapor attenuation factors derived for petroleum hydrocarbon compounds such as BTEX are generally lower than those obtained for chlorinated solvent chemicals, although the dataset for petroleum hydrocarbon sites is still relatively small, and there are case studies indicating limited degradation below buildings for shallow contamination sources (Johnson, 2006). For example, the groundwater-to-indoor air alpha's for chlorinated solvent chemicals typically range between 10^{-5} and 10^{-3}, whereas for petroleum hydrocarbons, the reported groundwater alpha's for BTEX chemicals are in most cases less than 10^{-4} (Hers et al., 2006).

Several regulatory agencies have incorporated bioattenuation in their framework for semi-site specific assessment of the vapor intrusion pathway. The draft Health Canada guidance incorporates a ten times (10X) reduction factor that can be applied to semi-site specific alpha's developed for non-degrading chemicals if there is a minimum separation distance between the building and contamination source and no significant capping effect that would reduce oxygen intrusion to below the building (Golder, 2004). Groundwater screening levels for vapor intrusion developed by the New Jersey Department of Environment (NJDEP), Massachusetts Department of Environmental Protection (MADEP), and San Francisco Regional Water Quality Control Board's (RWQCB) all incorporate a 10X reduction factor for BTEX chemicals. The rationale for the empirical adjustment factor incorporated in the above guidance is limited, although the Health Canada guidance includes a modeling study where a 2-D numerical model was used to assess the influence of aerobic biodegradation below a building for diffusive hydrocarbon and oxygen transport. This study suggested that for a weathered gasoline source, there would be sufficient oxygen to sustain aerobic biodegradation below a residential dwelling, for separation distances greater than approximately 3 to 4 m between the foundation and contamination source.

There are several models that include bioattenuation in the calculation of vapor attenuation factors. Johnson et al. (1998) present a modification of the Johnson and Ettinger (1991) algorithm that incorporates first-order biodegradation of hydrocarbon vapors within a single "dominant" soil layer. A second model by Johnson is an oxygen-limited hydrocarbon vapor migration attenuation screening model that incorporates diffusion and first-order biodecay within the unsaturated zone (unpublished, described in RISC 4.02 model documentation). An analytical solution for oxygen-limited biodegradation is coupled with an equation for mass flux through a building foundation and mixing of vapors inside the building, which enables a vapor attenuation factor to be

calculated. A unique feature of the oxygen-limited model is that it calculates an oxygen profile and a thickness of soil over which aerobic biodecay occurs. Abreu and Johnson (2005, 2006) present a multi-dimensional numerical model for simulation of vadose zone diffusion, advection, sorption and first-order biodecay. Other multi-dimensional models for vadose zone, vapor fate and transport have been developed by Hers et al. (2000) and Lahvis and Baehr (1996). Depending on the inputs, the above models may predict a bioattenuation factor that is much larger than the 10X reduction factor adopted by several regulatory agencies.

Modeling studies involving a detailed assessment of the influence of biodegradation on vapor attenuation factors and comparison to field data are relatively limited. This paper describes a new semi-analytical modification of the Johnson and Ettinger (1991) model that incorporates first- and zero-order oxygen-limited biodegradation over a dominant soil layer ("J&E-BIO model"). The advantages of the J&E-BIO model are that it is conceptually simple and through a semi-analytical solution, multiple soil layers and processes (e.g., first- and zero-order decay) can be readily evaluated. The objectives of this modeling study are to evaluate factors affecting hydrocarbon vapor biodegradation, and through model simulations and comparisons to field data, facilitate the development of regulatory guidance and reduction factors for aerobically degradable hydrocarbon compounds.

2.0 BIODEGRADATION RATE CONSTANTS FROM FIELD MEASUREMENTS AND COLUMN STUDIES

Studies relevant to this evaluation are where models have been used to back-calculate first-order biodegradation rate constants from soil vapor concentrations measured under natural field conditions or soil column tests designed to represent vadose zone conditions (e.g., Lahvis and Baehr, 1999; Hers el al., 2000, DeVaull et al., 2002). The estimated first-order aerobic biodegradation rates for several case studies are presented in Table 1. The rates implicitly assume that oxygen and hydrocarbon-degrading microbes are available in excess, and that only the hydrocarbon substrate is rate limiting.

The estimated biodegradation rates are highly sensitive to the effective diffusivity and moisture content. Back-calculated biodegradation rates are overestimated when there are thin un-quantified high moisture content layers (i.e., that are not included in the analysis), since these layers represent a partial barrier to diffusive transport. For cases where there are unresolved moisture content effects, fitted biodegradation rates are, in effect, lumped parameters. Due to the various sources of uncertainty, the estimated biodegradation rates should be considered order-of-magnitude estimates.

When evaluating first-order decay constants, it is essential that the type of constant (liquid- or gas-phase) be indicated. The equation to convert from a gas-phase (λ_g^1) to liquid-phase (λ_w^1) first-order decay constant is as follows:

$$\lambda_w^1 = \lambda_g^1 * H' / \theta_w \quad [1]$$

where H' is the dimensionless Henry's law constant and θ_w is the water-filled porosity (m^3/m^3).

The highest first-order decay constants were measured for aliphatic hydrocarbons (n-octane followed by n-decane) (Table 1). The decay constants for 2,2,4-trimethylpentane (0.65 to 15 hr^{-1}) were somewhat higher than those measured for BTEX compounds (0.033 to 1.2 hr^{-1}). Although the data is limited, the first-order decay constants for cyclohexane were similar to or slightly higher than those for BTEX compounds. The rate constants are approximately consistent with the relative degradation rates reported by Olson et al. (1999) for batch tests where the relative degradation rate were n-alkanes > aliphatics (composite solution light fraction) > aromatics > branched and cyclic alkanes > aromatics (composite solution heavier fraction).

There are a limited number of field studies where vertical vapor profiling has enabled the evaluation of BTEX or hydrocarbon vapor attenuation below buildings. At the former Chatterton petrochemical site (Delta, BC), there is extensive residual NAPL contamination and sand soils. The BTX vapor concentrations decreased over three orders-of-magnitude over a small depth interval (about 0.4 m), for cases where there was no significant advective soil gas transport. The best estimate first-order aerobic decay constants for BTX ranged from 0.5 to 1.2 hr^{-1}.

Fischer et al. (1996) reported that hydrocarbon vapor concentrations below an at-grade building (Alameda, CA) decreased sharply over a small vertical interval (0.1 to 0.7 m depth). The authors suggested that a partial physical barrier to vertical transport (i.e., high moisture content zone) in combination with biodegradation accounted for the steep gradient. Contrasting results were obtained at the Paulsboro, NJ site where vapor profiling was performed below and adjacent to a house with a basement (Laubacher et al., 1997). Testing approximately 0.6 m below the basement floor slab indicated elevated BTEX vapor concentrations and low O_2 concentrations (less than one percent). In contrast, BTEX vapor concentrations adjacent to the house (i.e., at the same depth) were two orders-of-magnitude lower, and O_2 levels were about 14 percent.

Several studies have involved monitoring at sites not covered by buildings. Ririe and Sweeney (1995) present data showing that BTEX vapor concentrations increased sharply with increasing depth. Complimentary geochemical data was obtained to demonstrate biodegradation was occurring. Ostendorf and Kampbell (1991) present similar data for a site contaminated with aviation fuel and derived kinetic biodegradation rate constants using a coupled diffusive hydrocarbon and O_2 transport model calibrated using field data. The GRACOS project was conducted by European researchers (Pasteris et al., 2002; Hohener et al., 2003; Gaganis et al., 2003; Maier et al., 2003). Their work included evaluation of first-order decay constants for a simulated fuel contamination source embedded in sandy soil, and several studies involving column tests.

Models that may more accurately simulate biodegradation than the first-order decay models that incorporate Monod kinetics (Bekins et al., 1998; DeVaull et al., 1997) or a combined model where first-order decay is assumed below a critical hydrocarbon

Table 1. Measured aerobic biodegradation rates from field and column studies

Site/Study	Chemical Class	Soil Type	Chemical	Concentration	1st-order decay rate (gas-phase) (hr^{-1})	Henry's Law Constant (dimension-less)	1st-order decay rate (aqueous-) phase) (hr^{-1})
Chatterton Hers et al. (2000)	BTX	F.-M.Sand	Benzene	10 mg/L	NC		0.5-2.0 (1.2)
			Toluene	20 mg/L	NC		0.3-1.5 (0.9)
			m &*p* -xylene	0.6 mg/L	NC		0.2-0.8 (0.5)
Alameda Fischer *et al.* (1996)	Gasoline	Sand	iso-pentane	50 g/m3			~2
Soil Columns (Sand) Jin et al. (1994)	Toluene	Pachappa Loam θ_w = 0.08 to 0.15	Toluene	11.1 - 140 mg/ L inlet	NC NC		0.33
Traverse City Ostendorf & Kampbell ('91)	Aviation Fuel	F. Sand	Total Hydrocarbon	100 to 10,000 ppm	NC NC		~0.01
California Ririe & Sweeney (1995)	Gasoline	Sand, thin clayey silt layers	Benzene	80,000 ppbV	NC		0.42
Perth, Australia Davis et al. (1998)	Gasoline	M.-C.Sand θ_w = 0.07 to 0.0.9 θ_a = 0.3 to 0.45	Total Hydrocarbon	10,000 ug/L	0.012 to 0.018		NC
Aerobic Microcosms Salanitro et al. (1988)	BTEX	Kalkaska Sand	BTEX	0.1 - 31 ppm	0.0072 to 0.014		NC
Convective Column Salanitro et al. (1989)	BTEX	Kalkaska Sand	BTEX	up to 500 ppm	> 0.029		NC
Beufort, S. Carolina Lahvis and Baehr (1999)	Gasoline	Silt and fine-grained Sand	Benzene	Near water table	0.0030 to 0.013	0.217	0.007 to 0.028
			Toluene		0.0038 to 0.013	0.244	0.009 to 0.032
			Ethylbenzene		0.0045 to 0.013	0.26	0.012 to 0.034
			Xylenes		0.0042 to 0.013	0.26	0.011 to 0.034
Large-scale Lysimeter Pasteris et al. (2002)	Simulated Gasoline (13 fuel components & tracer (CFC-11)	Sand Lake Geneva, Rhone River 2.5 m high lysimeter θ_w = 0.05 θ = 0.41 f_{oc} = 0.002 k_a = 2 to 4 10^{-12} m^2	n-octane	0.1 m NAPL layer	0.21 to 0.36	93.5	392 to 673
			n-decane		0.21	7.7	32.34
			n-dodecane		0.11	9.6	21.12
			n-hexane		0.017	36	12.24
			methylcyclopentane		0.0062	14.8	1.84
			methylcyclohexane		0.017	2.78	0.95
			cyclohexane		0.0083 to 0.033	6.6	1.1 to 4.2
			2,2,4-trimethylpentane		0.0042 to 0.0062	124	10.4 to 15.3
			toluene		0.13	0.244	0.63
			MTBE		<0.0021	-	-
Column Study Hohener et al. (2003)	Simulated Gasoline (13 fuel com-ponents & tracer (CFC-11)	Sand Lake Geneva, Rhone River θ_w = 0.118 1.4 m by 8.1 cm column	n-octane	End of column contact fuel	0.21	93.5	166.31
			n-decane		0.56	7.7	36.71
			n-hexane		0.011	36	3.31
			methylcyclopentane		0.0042	14.8	0.52
			methylcyclohexane		0.0067	2.78	0.16
			cyclohexane		0.0029	6.6	0.16
			2,2,4-trimethylpentane		0.0038	124	3.93
			toluene		0.055	0.244	0.11
			n-pentane		<0.00042	49.2	<0.18
			1,2,4-trimethylbenzene		0.2075	0.28	0.49
			MTBE		<0.00042	-	-
Field Study Airbase Vaerlose Denmark Gaganis et al. (2003) Maier et al. (2003) Inverse modeling using MOFAT & MIN3D	Simulated jet fuel (14 compounds)	Sand θ_w = 0.05 to 0.1 θ_w = 0.08 for calculations	n-octane	N/A	0.044 to 0.045	93.5	66 to 68
			n-decane		0.15 to 0.18	7.7	14 to 17
			cyclopentane		0.00083	9.6	0.10
			n-hexane		0.00017 to 0.002	36	0.08 to 0.9
			methylcyclopentane		0.0075	14.8	1.39
			methylcyclohexane		0.0042	2.78	0.15
			3-methylpentane		0.00042	69.4	0.36
			2,2,4-trimethylpentane		0.00042 to 0.0062	123.6	0.65 to 9.6
			Benzene		0.026 to 0.081	0.217	0.070 to 0.22
			Toluene		0.011 to 0.019	0.244	0.033 to 0.030
			m-xylene		0.069	0.26	0.22
			1,2,4-trimethylbenzene		0.11	0.28	0.39

NC = not calculated due to insufficient information

concentration, and a zero-order decay model is assumed when the concentration exceeds the critical concentration (Hers et al., 2000). Above the critical concentration, the hydrocarbon decay rate stays constant since the hydrocarbon concentration is no longer rate-limiting. Although there is considerable scatter in the data, there appears to be evidence for first-order decay at lower concentrations and zero-order decay at higher concentrations from the field studies and column tests presented in Figure 1 (from DeVaull et al, 1997), which indicate that the increase in degradation rate (per unit volume) tails of at higher pore-water concentrations.

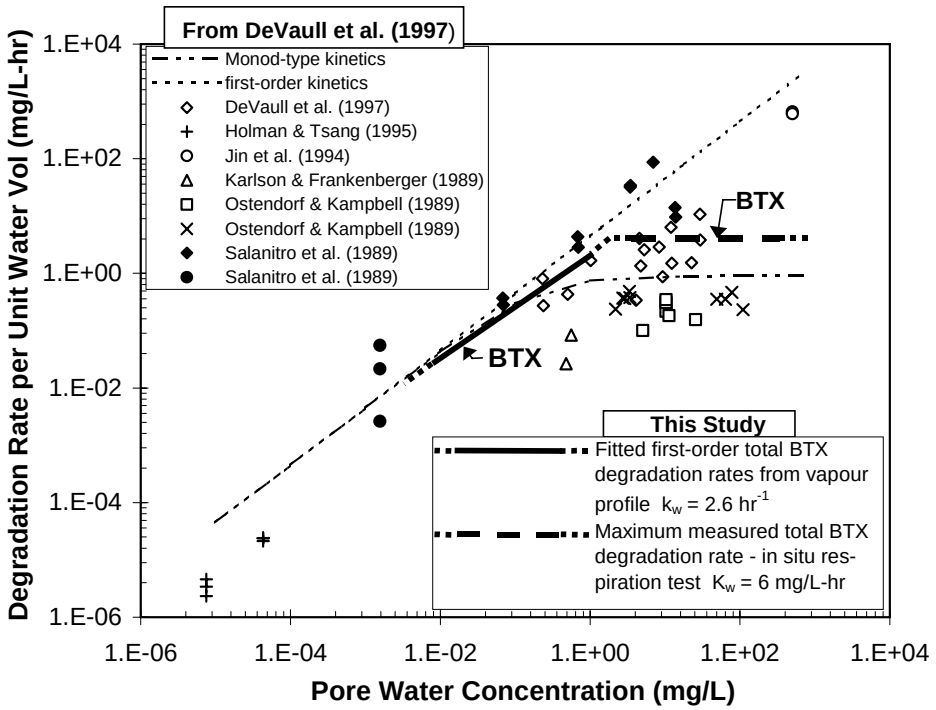

Figure 1: Comparison of field degradation rates to published data in DeVaull et al. (1997) (used with permission).

3.0 MODEL THEORY AND EQUATIONS

The Johnson and Ettinger (1991) model was modified to incorporate oxygen-limited first-order or zero-order biodegradation through a semi-analytical numerical solution using the SOLVER routine in Excel (J&E-BIO model). First- or zero-order biodegradation is limited to a single dominant soil layer (Johnson et al., 1998). While the model simulates transport through up to eight soil layers, to simplify the discussion, the diffusive mass flux equations for a three-layer soil system (Layers 1 to 3), with biodegradation also occurring over the middle layer (Layer 2) (Equations 2 to 8). The flux continuity equations require that the upward diffusive flux in a soil layer equal to the diffusive flux and biodegradation flux in the overlying soil layer (e.g., Equation 2).

*Flux continuity between **Layer 1** and **Layer 2: Sub-layer 1** (2,1)*

$$A_b\, D_1\, (C_S - C_{2,1})/L_1 = A_b\, D_{2,1}\, (C_{2,1} - C_{2,2})/L_{2,1} + A_b\, G_{2,1}\, L_{2,1}\, UCF_1 \quad [2]$$

*Flux continuity between **Layer 2 sub-layers** (where n is equal to number of sub-layers)*

$$\text{For i = 1 to n} \quad A_b\, D_{2,i}\, (C_{2,i} - C_{2,i+1})/L_{2,i} = A_b\, D_{2,i}\, (C_{2,i} - C_{2,i+1})/L_{2,i} + A_b\, G_{2,i}\, L_{2,i}\, UCF_1 \quad [3]$$

$$\text{Layer 2,1} \quad A_b\, D_{2,1}\, (C_{2,1} - C_{2,2})/L_{2,1}\, A_b = A_b\, D_{2,2}\, (C_{2,2} - C_{2,3})/L_{2,2} + A_b\, G_{2,2}\, L_{2,2}\, UCF_1$$
$$\text{Layer 2,2} \quad A_b\, D_{2,2}\, (C_{2,2} - C_{2,3})/L_{2,2}\, A_b = A_b\, D_{2,3}\, (C_{2,2} - C_{2,4})/L_{2,3} + A_b\, G_{2,3}\, L_{2,3}\, UCF_1$$

*Flux continuity between **Layer 2: Sub-layer n** (2,n) and **Layer 3***

$$A_b\, D_{2,n}\, (C_{2,n} - C_3)/L_{2,n} = A_b\, D_3\, (C_3 - C_4)/L_3 \quad [4]$$

*Flux continuity between **Layer 3** and **Layer 4 (foundation)***

$$A_b\, D_3\, (C_3 - C_4)/L_3\, A_b = A_b\, D_4\, (C_4 - C_{in})/L_4\, \eta + Q_s\, C_4\, UCF_2 \quad [5]$$

Equation for mixing of vapors in indoor air

$$C_{in} = [A_b\, D_4\, (C_4 - C_{in})/L_4\, \eta + Q_s\, C_4\, UCF_2] / Q_{build} \quad [6]$$

Constraints

$$\text{For i = 1 to n} \quad \text{If } C_{2,i} < C_{crit} \text{ then } G_{2,i} = C_{2,i}\, \lambda_w^{\,1}\, \theta_{w\,2,\,i}\, /H' \text{ (first-order)}$$
$$\text{else } G_{2,i} = \lambda_w^{\,0} \text{ (zero-order)} \quad [7]$$

$$Bio = \sum \text{ i to n } [G_{2,i}\, A_b\, L_{2,i,}]$$

$$\text{If } Bio <= F_o \text{ then analysis is complete}$$
$$\text{else reduce } \lambda_w^{\,1} \text{ or } \lambda_w^{\,0} \text{ until } Bio = F_o \quad [8]$$

Where D_1 to D_3 is the effective diffusion coefficient (m^2/s), D_4 is the effective diffusion coefficient of the dust-filled cracks of the foundation (m^2/s), C is the soil vapor concentration (mg/m^3), C_S is the source concentration (mg/m^3, and assumed to be constant), G is the biodegradation rate (mg/m^3-hr), L is the thickness of the soil layer (m), A_b is the subsurface area for vapor intrusion (m^2), i is the sub-layer subscript, Q_s is the soil gas advection rate (L/min), Q_{build} is the building ventilation rate (L/min), F_o is the maximum flux of hydrocarbon that can be degraded through aerobic degradation (mg/s), C_{in} is the indoor air concentration (mg/m^3), η is the crack ratio (dimensionless), C_{crit} is the critical concentration separating zero- and first-order decay, UCF_1 is a unit conversion factor (1/3,600 hr/sec), and UCF_2 is a unit conversion factor (1/60,000 min-m^3/sec-L).

The above equations are solved iteratively using SOLVER. Equations 7 and 8 are solved using functions in EXCEL. The initial mass of hydrocarbon degraded is calculated using

the user-defined first-order decay constant. If this mass exceeds the maximum flux that can be aerobically degraded (F_o), then λ_w^1 or λ_w^0 is iteratively reduced until the sum of the biodegradation flux across all layers equals F_o. If the initial mass of hydrocarbon degraded is less than F_o using the initial value of λ_w^1 or λ_w^0, the solution is complete. The calculation procedure for the F_o parameter is presented below in Section 6.1.

For the purposes of this paper, the above equations were solved for eight soil layers. First-order biodegradation was limited to a single dominant soil unit comprised of 30 sub-layers (n = 30 in equation 3). The model predictions for the J&E-BIO model (no oxygen limitation case) were compared to the RISC 4.02 model (Figure 2) for a three-layer scenario. The results indicate a good comparison between the two models with a maximum difference in the vapor attenuation factor of 5 percent. The difference between the two models decreases as the number of sub-layers was increased. While more sub-layers can easily be added to the spreadsheet to improve the accuracy of the numerical solution, for the purposes of this assessment, model equation formulation with n equal to 30 was considered adequate for screening purposes.

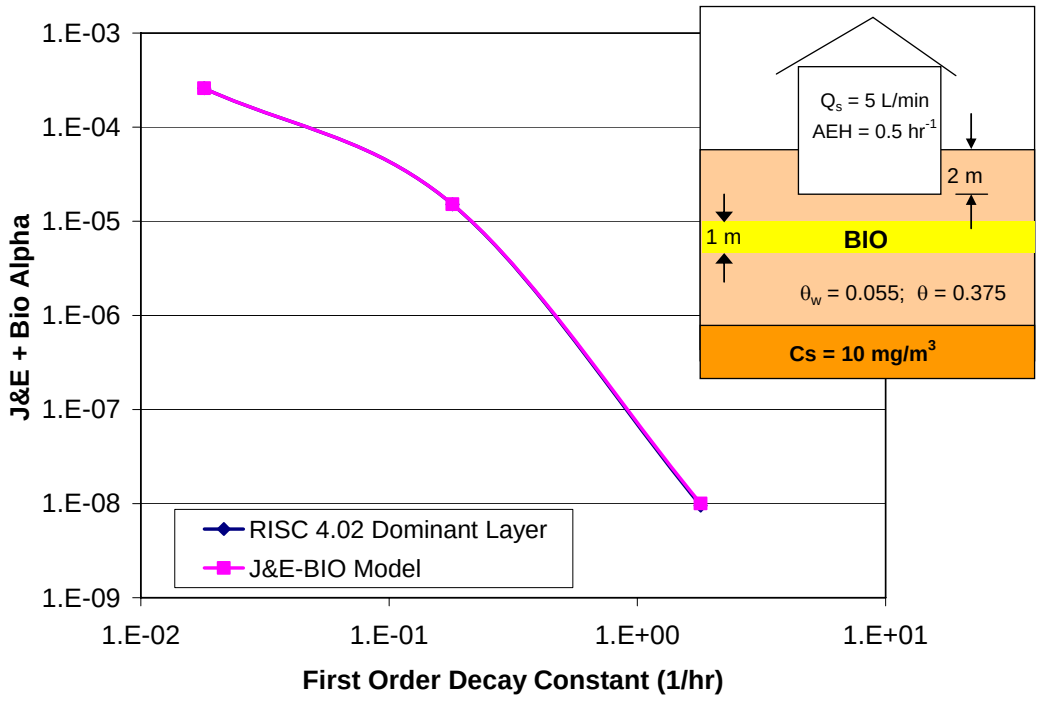

Figure 2. Comparison of J&E-BIO and RISC 4.02 Model Predictions

4.0 BENCHMARKING OF J&E-BIO MODEL

The J&E-BIO model provides a useful tool for rapid assessment of the contribution of bioattenuation on overall vapor attenuation. However, the model is limited to one-dimensional transport and the way in which oxygen-limited first-order attenuation is modeled is approximate. For this reason, the model was benchmarked against the results of the 3-D modeling study published by Abreu and Johnson (2006), which represents the

most comprehensive numerical modeling study for vapor intrusion conducted to-date. Unless otherwise indicated, the J&E-BIO model simulations that follow in this paper use the same input parameters as those used by Abreu and Johnson (2006).

The three-dimensional model developed by Abreu and Johnson (2005, 2006) simulates diffusion, gas-phase advection through building depressurization and oxygen-limited first-order biodecay. For most model simulations, homogeneous soil properties and a vapor source above the water table were assumed (i.e., no capillary fringe). The total hydrocarbon vapor concentrations at the source ranged between 2 and 200 mg/L, which approximates the range of vapor concentrations expected above a weathered diesel (2 mg/L) and weathered gasoline source (200 mg/L). The first-order decay constants input into model simulations ranged between 0.018 and 1.8 hr^{-1}. Based on the literature values previously presented, this range of first-order decay constants is representative of those expected for aerobic biodecay of most hydrocarbon vapors within the unsaturated zone. The results of Abreu and Johnson (2006) for a first-order biodecay rate of 0.18 hr^{-1} (i.e, mid-point value) are reproduced in Figure 3.

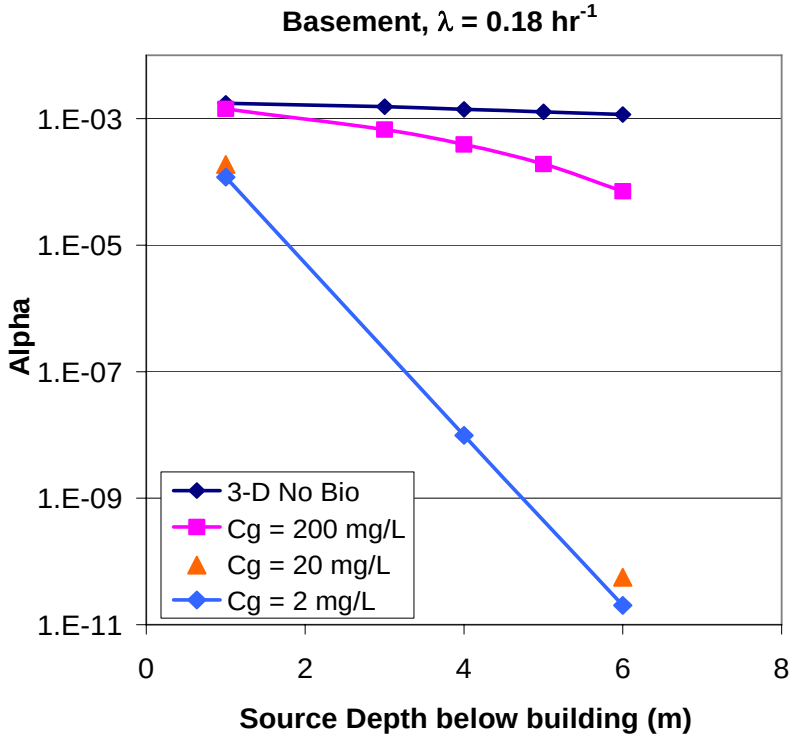

Figure 3. Model-predicted alpha for Abreu-Johnson 3-D Model (from Abreu and Johnson, 2006)

In Figure 4, the same modeling results are presented in terms of a reduction factor (RF), which is the ratio of the alpha without biodecay divided by the alpha with biodecay. As shown, the RF is strongly influenced by the source vapor concentrations. For a source concentration equal to 200 mg/L, a separation distance of over 5 m between the building foundation and source is required before a RF of ten is obtained (i.e., for basement

residential scenario). For source concentrations of 2 and 20 mg/L, there are much larger RFs at even smaller separation distances.

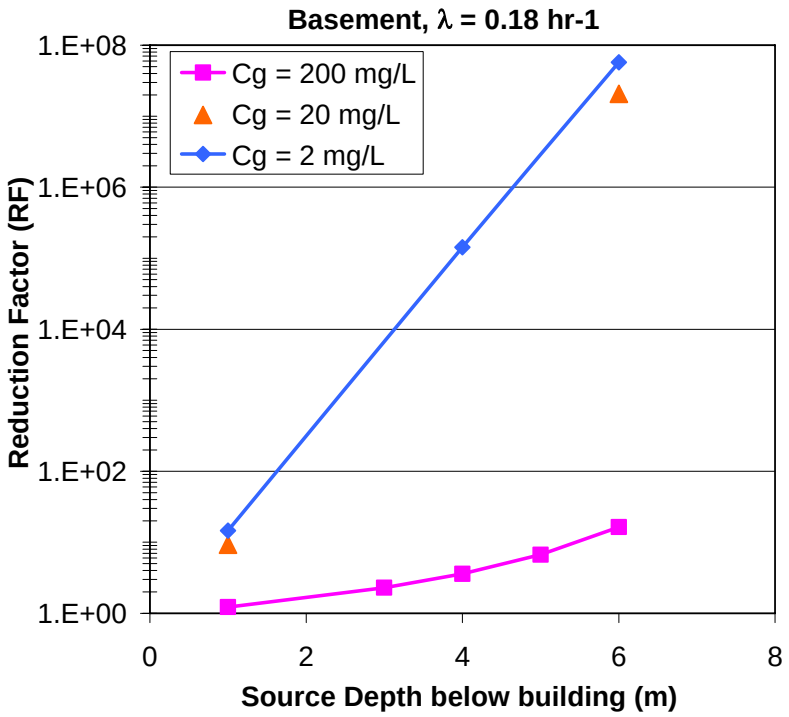

Figure 4. Model-predicted Reduction Factor (RF) for Abreu-Johnson 3-D Model (adapted from Abreu and Johnson, 2006)

5.0 J&E-BIO DOMINANT LAYER MODEL SIMULATIONS (NO OXYGEN LIMITATIONS)

5.1 Uniform Soil Moisture Content

The J&E-BIO model was compared to the Abreu and Johnson (2006) model results for a basement scenario, a first-order biodecay rate of 0.18 hr^{-1} and uniform soil moisture content (Figure 5). The thickness of the dominant layer was equal to 1/3 the distance from ground surface to the vapor contamination source, except for shallow contamination cases where the thickness was less (Table 2). The J&E-BIO dominant layer model simulations indicate slightly higher alpha values compared to the 3-D model simulations for low source concentration scenarios (Cs = 2 and 20 mg/L) where there were no significant oxygen limitations for biodegradation below the building. In contrast, the dominant layer alpha values were much lower than the 3-D model results for high source strength (Cs = 200 mg/L). The model simulations highlight that a dominant layer model that does not include consideration of oxygen limitations may under predict vapor intrusion when there are high source hydrocarbon concentrations.

Table 2. Input Parameters for J&E-BIO Modeling

Vapor source depth bgs (D) (m)	Vapor source founda-tion distance (m)	Thickness 1st-order biodecay layer (T = D/3) (m)	Distance biodecay layer foundation (B) (m)	Diffusion path length O_2 flux (L_{O2}) (m)	Width for O_2 flux (W) (m)	Area for O_2 flux[1] (m^2)	Max HC degrad-ed (mg/s)	Max HC degraded - uniform sand (mg/s)	Max HC degraded - poor quality concrete (mg/s)	Max HC degraded - good quality concrete (mg/s)
3.0	1.0	0.33	0.00	3.5	1.5	69	4.11	4.11	3.78	0.77
4.0	2.0	0.67	0.00	3.92	2.0	97	5.06	5.06	4.70	1.05
5.0	3.0	1.33	0.00	4.33	2.5	125	6.01	6.01	5.62	1.34
6.0	4.0	2.00	0.00	5.0	3.0	156	6.50	6.50	6.13	1.61
7.0	5.0	2.33	0.33	5.67	3.5	189	6.95	6.95	6.60	1.89
8.0	6.0	2.67	0.67	6.33	4.0	224	7.37	7.37	7.04	2.17

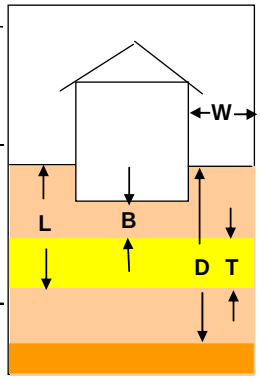

Notes:
1. Area O_2 flux = (10+W)*W*4 L_{O2} = L + 1 m
2. Maximum HC flux degraded equal to O_2 flux divided stochiometric ratio (3)
3. O_2 flux = A_{O2} * D_{O2}^{eff} * ΔC_{O2} / L_{O2}
4. Uniform sand θ_w = 0.07, θ = 0.35

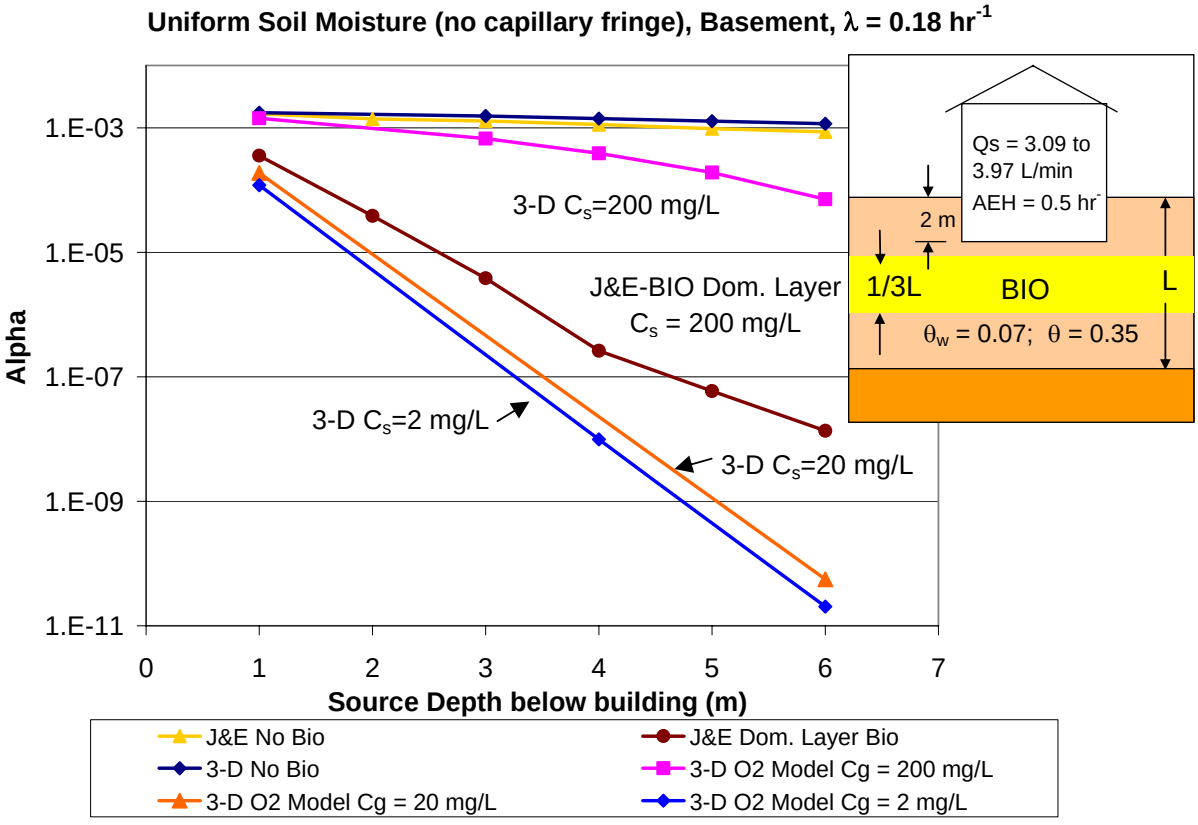

Figure 5. Comparison J&E-BIO Dominant Layer to Abreu-Johnson 3-D Model

The results of the 3-D model were also compared to the Johnson and Ettinger (1991, i.e. 1-D) model for identical input parameters and no biodegradation. The comparison, shown in Figure 6, indicates that the resultant difference between the 3-D and 1-D model increases with increasing depth. For a 6 m distance from the building to the vapor contamination source, the difference is approximately 30 percent. The 3-D model

predicts the higher alpha's since the contamination source extends laterally beyond the building footprint and since vapors are drawn from beside the building.

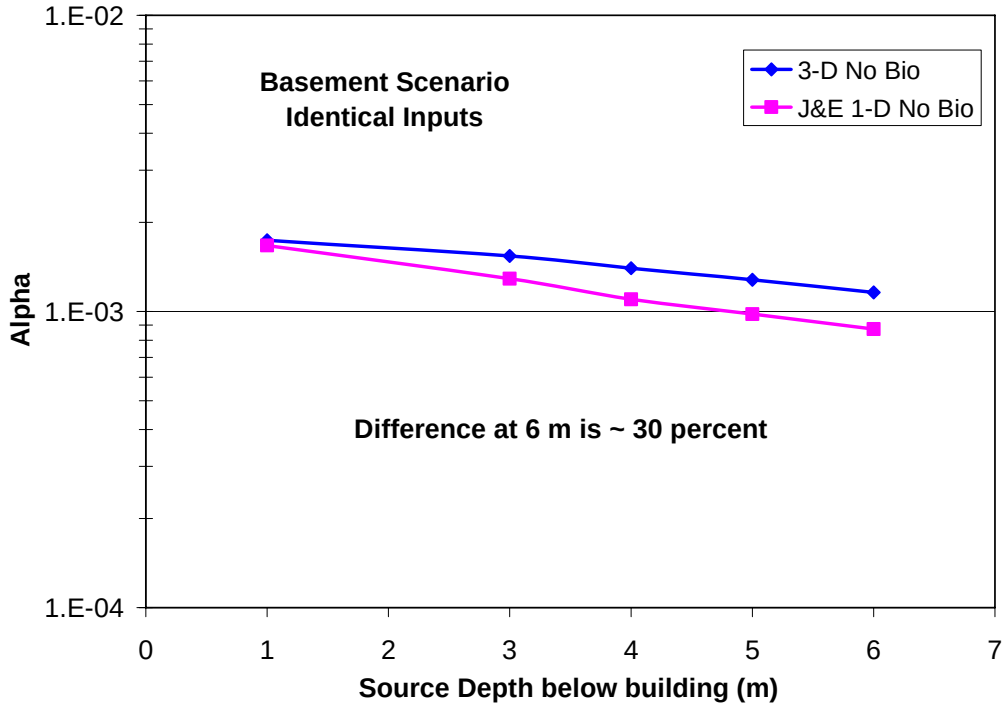

Figure 6. Comparison of 3-D model and Johnson and Ettinger (1-D) model predictions for identical inputs (Table S-3 in Abreu and Johnson (2006); no biodegradation case)

5.2 Variable Soil Moisture Content (Capillary Fringe Scenario)

The influence of variable moisture content within the capillary fringe and biodegradation layer were evaluated using the J&E-BIO model for the following cases:

1. Uniform soil moisture (no capillary fringe) and no biodegradation.
2. Uniform soil moisture (no capillary fringe) and first-order biodegradation within a dominant soil layer.
3. Five-layer capillary fringe and no biodegradation.
4. Five-layer capillary fringe and first-order biodegradation.

For a dissolved groundwater source, the model simulations assumed a variable water-filled porosity profile for the capillary fringe. The Van Genuchten (VG) model for the water retention curve and VG curve-fitting parameters published by Schaap and Lej (1998) for a US Soil Conservation Service (SCS) sand soil texture were used to estimate the water-filled porosity profile (Hers et al, 2003). The capillary fringe was divided into five layers (Figure 7). The single layer assumption used for the development of the

USEPA Vapor Intrusion Guidance (USEPA, 2002) is also shown for comparison. The distance between the building and vapor source for all scenarios was 3 m. The J&E input parameters were identical to those assumed by Abreau and Johnson (2006) and those used to generate Figure 6, except that the water-filled and total porosities values were those estimated for a U.S. Soil Conservation Sand (SCS) sand.

The model simulation results illustrate the significant influence that both variable water-filled porosity (capillary fringe) and biodegradation have on the predicted soil vapor profiles and alpha values (Figure 8). The combined effect of the capillary fringe and biodegradation (λ = 0.18 hr^{-1}) over a 1.33 m thick soil layer are dramantic, with a predicted alpha ($2.3x10^{-7}$) that is almost four orders-of-magnitude less than the alpha predicted for a uniform soil and no biodegradation.

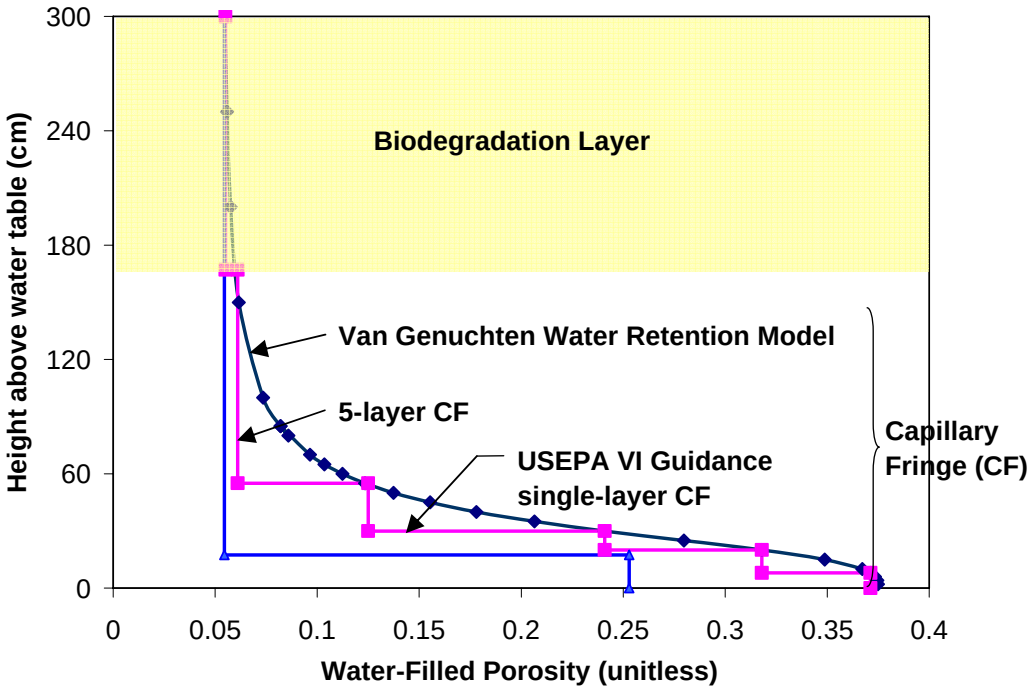

Figure 7. Soil Moisture Model

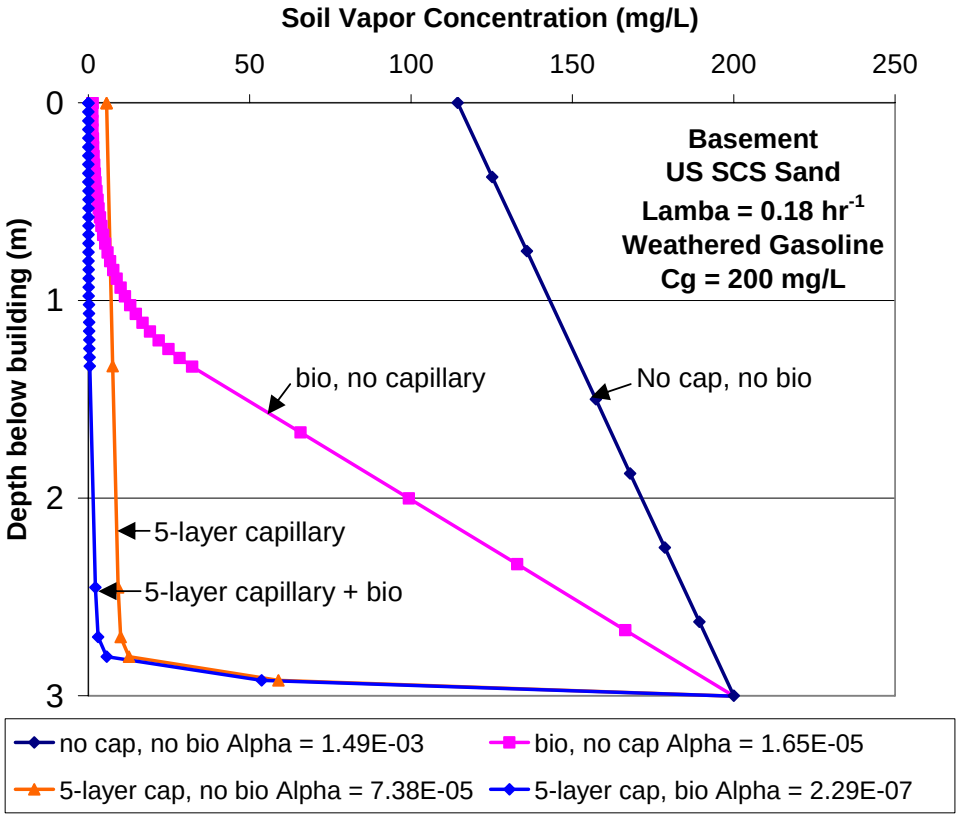

Figure 8. Influence Capillary Fringe and First-order Biodegradation on Vapor Profile

6.0 J&E-BIO DOMINANT LAYER O2-LIMITED MODEL SIMULATIONS

The J&E-BIO model may be used to evaluate the influence of oxygen-limitations by adjusting the first-order decay constant such that the mass of hydrocarbon degraded is less than or equal to the maximum theoretical hydrocarbon degraded through aerobic biodegradation (equation 8). The J&E-BIO oxygen limited biodegradation model is first used below to predict an alpha for the base case scenario involving a uniform soil moisture profile and identical input parameters to those assumed by Abreu and Johnson (2006). For the base case simulations, a one-dimensional model for oxygen diffusion is utilized to predict available oxygen for hydrocarbon biodegradation. Next, several different model scenarios were run to evaluate the influence of different factors on biodegradation (capillary fringe, surface cap, wind and barometric pressure).

6.1 Diffusion Model for Oxygen Flux

The oxygen flux was estimated using a one-dimensional diffusion model, as follows:

$$O_{2\text{-Flux}} = A_{O2} * D_{O2}^{eff} * (C_{O2\,i} - C_{O2f}) / L_{O2} \qquad [9]$$

Where $O_{2\text{-Flux}}$ is the oxygen flux (mg/s), A_{O2} is the area over which oxygen diffusion occurs (m^2), D_{O2}^{eff} is the effective diffusion coefficient of oxygen in soil (m^2/sec), $C_{O2\,i}$ is the initial oxygen concentration at ground surface (20.9% or 279 mg/L_{vapor}), C_{O2f} is the final oxygen concentration below the building assuming there is a threshold below which no additional oxygen can be consumed by microbes (1% or 13.7 mg/L_{vapor}) and L_{O2} (m) is the distance over which oxygen diffusion occurs. The D_{O2}^{eff} was estimated using the Millington-Quirck (1961) relationship. The maximum flux of hydrocarbon degraded through aerobic degradation (F_o, previously defined in equation 8) was estimated based on the stoichiometric relationship for hydrocarbon degradation, as follows:

$$F_o = O_{2\text{-Flux}} / SR \qquad [10]$$

where SR is the stoichiometric ratio of moles of oxygen to hydrocarbon degraded, taken to be three for model simulations presented in this paper. The area (A_{O2}) and diffusion distance (L_{O2}) were estimated assuming oxygen migration occurs beside and below the building, but not through the building foundation (i.e., conservative assumption), and that these values increase with increasing depth below ground surface. This is a reasonable assumption since as the distance to the contamination source increases there will be greater opportunity for lateral migration of oxygen from beside the building to below the building, and thus a greater area over which oxygen transport will occur. Nevertheless, it is recognized that the one-dimensional model and inputs chosen for oxygen diffusion are only approximate.

6.2 J&E-BIO O_2-Limited Model Base Case Simulations (Uniform Soil)

The J&E-BIO model was used to predict alpha for a scenario involving oxygen-limited first-order biodecay over a dominant soil layer. For the base case simulations, the input parameters for the J&E model were identical to those previously assumed in this paper. A uniform soil moisture profile and a weathered gasoline source with vapor concentration equal to 200 mg/L were assumed. The maximum hydrocarbon flux (F_o) that can be aerobically degraded ranges from 4.1 to 7.4 mg/s (Table 2).

The base case J&E-BIO oxygen-limited model simulations indicate alpha values that follow the same trend as those predicted by the Abreu and Johnson 3-D model (Abreu and Johnson, 2006) (Figure 9). The J&E-BIO alpha's are slightly higher (i.e., more conservative) than those predicted using the 3-D model, which is desirable for bench-marking purposes and subsequent simulations where input parameters are varied.

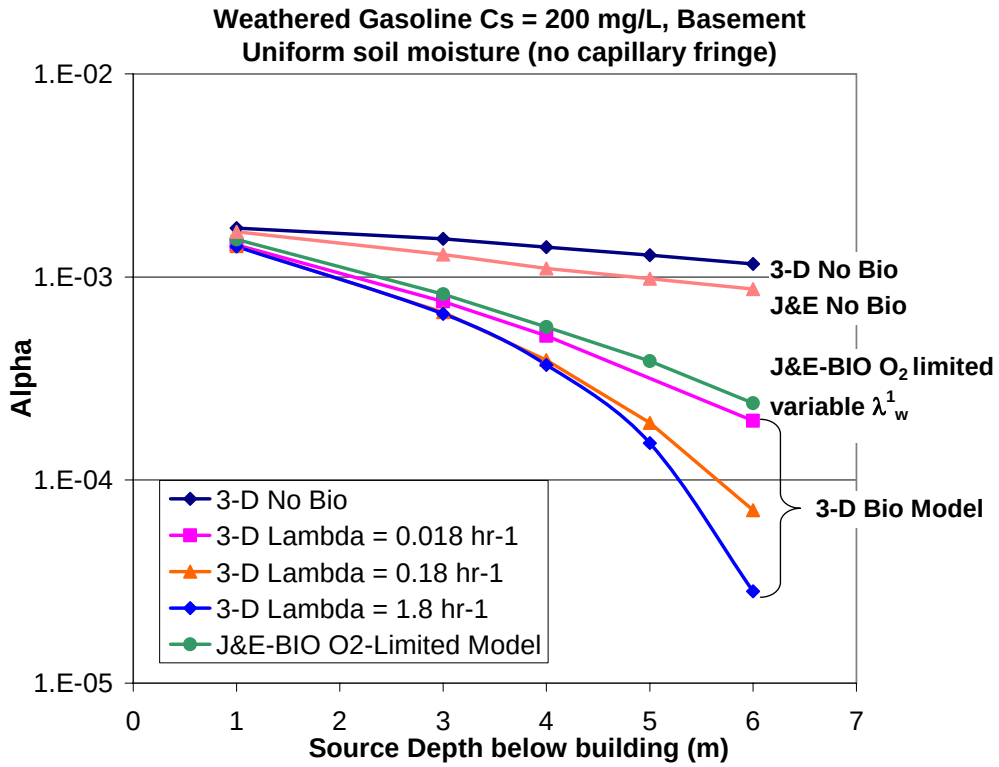

Figure 9. J&E-BIO model oxygen-limited simulations for base case scenario

6.3 J&E-BIO O_2-Limited Model – Influence Capillary Fringe

The evaluation of the capillary fringe scenario assumed a five-layer soil moisture profile for a SCS sand soil. The J&E-BIO oxygen-limited model simulations for this scenario indicate the alpha's for a five-layer capillary fringe profile are three to four orders-of-magnitude lower than those for a uniform soil moisture profile for the scenario modeled, which was a residential basement and weathered gasoline source (Figure 10). An important finding for the five-layer capillary fringe scenario was that oxygen was not limiting. For the simulation, oxygen supply exceeded the oxygen demand based on the reduced hydrocarbon flux through the capillary fringe, implying that re-aeration beneath a residential foundation can be substantial even in the presence of active biodegradation.

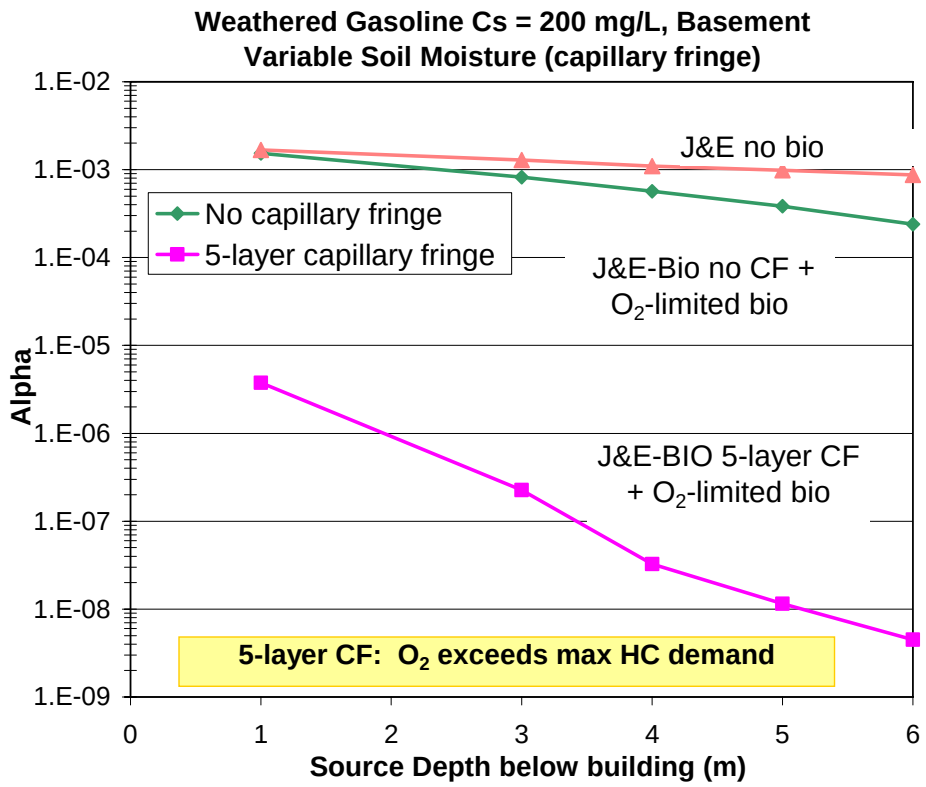

Figure 10. J&E-BIO model oxygen-limited simulations for capillary fringe scenario

6.4 J&E-BIO O_2-Limited Model – Influence Surface Capping Layer

Asphalt or concrete paved surfaces located besides a building may reduce the flux of oxygen to below the building. The oxygen flux through lawns may also be reduced relative to coarser soils due to the higher moisture content within surface topsoil. Asphalt properties vary widely, for example, the air-filled porosity typically varies between 4 and 8 percent; however, for porous pavements which are designed to promote infiltration, the air-filled porosity can be as high as 50 percent. However, the interconnected or effective air-filled porosity values for asphalt are difficult to determine and no data on effective diffusion coefficients for asphalt could be found. There is data on the air permeability of asphalt, for example, a study by Li et al. (2004) indicated that the air permeability ranged from $4x10^{-13}$ to $9x10^{-13}$ m^2 for most samples tested. This permeability range is comparable to that for silty sand to sandy silt. There are several studies where an effective diffusion coefficient for radon migration through concrete has been measured; three studies are summarized in Table 3. Based on these studies, a range of effective radon diffusion coefficients for good and poor quality concrete were estimated (10^{th} and 90^{th} coefficients in Table 3). For the modeling described below, the radon diffusion coefficient was first used to obtain a tortuosity factor, which is independent of chemical properties, which was in turn used to calculate an oxygen diffusion coefficient.

The J&E-BIO oxygen-limited model was used to evaluate the influence of reduced oxygen diffusion through a 0.2 m concrete capping layer for good and poor quality concrete. Oxygen diffusion through concrete and soil was limited to that occurring from beside the building. The concrete surface cap is underlain by uniform sand to the water table (i.e., no capillary fringe). All other parameters are identical to the J&E-BIO oxygen-limited base case simulations. The maximum hydrocarbon flux that can be aerobically degraded is summarized in Table 2.

The J&E-BIO model simulations for the surface barrier scenario indicate that using the assumed diffusion coefficient for good quality concrete, the model predicts significant oxygen limitations below the slab and little difference relative to the no biodegradation case. When a poor quality concrete surface is modeled, the results are similar to the homogeneous sand case (i.e., no barrier). The large difference in the results for the two scenarios indicates that the quality of the barrier may have a significant effect on oxygen diffusion below buildings. The oxygen diffusion rate through asphalt is expected to be higher than for concrete.

Table 3. Summary of Measured Radon Diffusion Coefficients for Concrete

Concrete Condition	Diffusion coefficient		Permeability		Porosity	Reference
	Minimum (cm^2/sec)	Maximum (cm^2/sec)	Minimum (cm^2)	Maximum (cm^2)		
	4.96E-04	1.43E-03	1.35E-12	4.97E-12	0.12 - 0.2	Renken & Rosenberg ('95)[1]
	1.69E-05		-	-	0.06	Culot et al. (1976)
Heavy concrete	6.80E-06		-	-	0.1	Folkerts et al. (1984).
	3.34E-04	6.01E-04	-	-	0.07 - 0.32	Siotis and Wrixon (1984)
	1.69E-04	4.70E-04	-	-	0.11 - 0.13	Stranden (1983).[2]
	1.80E-04	4.60E-03	8.00E-13	8.70E-12	0.17 - 0.26	Rogers & Nielson (1992).[3]
Slab samples	2.10E-04	1.10E-03	-	-	-	Rogers et al. (1994).
Test cylinders	1.10E-03	5.20E-03	-	-	-	Rogers et al. (1994).
Uniform slab (137 to 171d)[4]	5.90E-04	7.10E-04	-	-	-	Nielson et al. 1997.
Uniform slab (832d)	2.50E-03		-	-	-	Nielson et al. 1997.
Masonry block (177 to 237d)	1.30E-02	4.50E-02	-	-	-	Nielson et al. 1997.
Tension bars passive (190-199d)	6.70E-04	7.50E-04	-	-	-	Nielson et al. 1997.
Tension bars passive (839d)	1.60E-03		-	-	-	Nielson et al. 1997.
Pipe penetration undisturbed (204-226d)	6.40E-04	8.50E-04	-	-	-	Nielson et al. 1997.
Pipes removed,rotated & reinserted (233-259d)	7.40E-04	1.50E-03	-	-	-	Nielson et al. 1997.
Pipes with 0.24 mm gap (270d)	1.20E-02		-	-	-	Nielson et al. 1997.
Pipe gaps caulked at top (841-848d)	2.20E-03	2.30E-03	-	-	-	Nielson et al. 1997.
			-	-	-	Nielson et al. 1997.
Acylic surface sealant (253d)	8.10E-04		-	-	-	Nielson et al. 1997.
Fibed asphalt coating (852d)	3.30E-04		-	-	-	Nielson et al. 1997.
10th percentile	**1.8E-04**					
90th percentile	**5.2E-03**					

Notes:
1. Three samples
2. Reported uncertainty of 100% in values.
3. Diffusion coefficients measured using transient method formulated to provide steady state coefficient.
4. Days refers to number of days test conducted after concrete constructed.

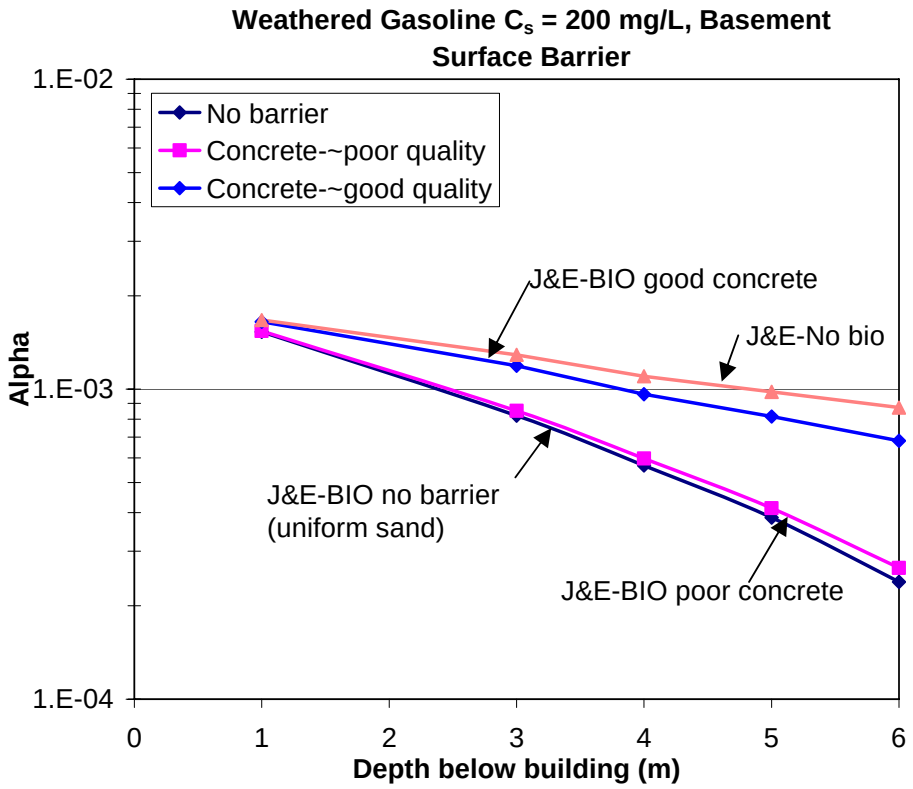

Figure 11. J&E-BIO model oxygen-limited simulations for surface barrier scenario

6.5 Influence of Wind

The force of wind on a building will result in positive pressure on the windward side of the building and a negative pressure on the leeward side of the building. The difference in the pressure between the windward and leeward side of the building will result in lateral soil gas flow below the building and movement of air into foundation subsoils. The pressure generated by wind at the base of a building can be estimated from the equation for Bernoulli pressure (Fischer et al., 1996):

$$\Delta P = K * (0.5\ \rho_a\ v^2) \qquad [11]$$

where ΔP is the pressure (Pa), K is an empirical factor (typically 0.2 to 0.3), ρ_a is the density of air (1.19 kg/m^3 at 20^{o}C), and v is the wind speed (mph). The flow rate of air moving through soil can be estimated using Darcy's equation:

$$Q = T * W * (k_a/\mu * 2\Delta P/\Delta X) \qquad [12]$$

Where Q is the air-flow rate (m^3/day), T is the thickness of soil (m), W is the width of the building (m), k_a is the soil-air permeability (m^2), μ is the viscosity of air (1.81x10^{-5} Pa-s at

20^oC), and ΔX is the length of the building parallel to the prevailing wind direction (m). The oxygen flux ($MO_{2)}$ and hydrocarbon mass degraded ($F_{o)}$ through wind-induced flow are calculated as follows:

$$MO_2 = Q\ \rho_a\ 0.209 \qquad F_o = MO_2 / SR \qquad [13]$$

The MO_2 was calculated for a typical residential scenario (10 m by 10 m building), moderate wind speed (v = 10 mph), and a 0.5 m thick sand fill layer below the building with k_a equal to 10^{-11} m^2 (sand). Assuming a K value equal to 0.25, a F_o of 0.14 mg/s is obtained. The wind-induced aerobic hydrocarbon degradation rate is more than one order-of-magnitude less than the baseline (diffusion) case (4.1 to 7.4 mg/s). The above calculation indicates that wind is likely less important than diffusion for oxygenation (i.e reaeration) of soil below buildings at many sites.

6.6 Barometric Pressure Effects

Changes in barometric pressure will influence subsurface soil gas conditions, which in turn, may both increase the potential for upward migration of hydrocarbon vapors, and downward movement of air. "Barometric pumping," caused by cyclic changes in atmospheric pressure, causes a "piston-like" force on soil gas, causing compression of soil gas when the air pressure increases, and expansion when it decreases. This may result in a cyclic up and down movement of contaminant vapours in the affected interval. Typically, the maximum variation in barometric pressure is about three percent over a 24-hour period (Massman and Farrier, 1992). Assuming gas compression according to the ideal gas law, atmospheric air will be pushed into surface soil to a depth up to about three percent of the total depth of the unsaturated zone. For a 10 m thick homogeneous unsaturated soil column, this means that the top 0.3 m of soil would be affected by the complete barometric flushing of soil gas.

While the flushing of near surface soil gas will reduce the diffusion path length for hydrocarbon and oxygen diffusion, a potentially more important process may be enhanced dispersion caused by soil gas advection. Parker (2003) in examining this process defined a total effective diffusion-dispersion coefficient, as follows:

$$D_{total} = D_{disp} + D_{diff} \qquad [14]$$

$$A_l = \beta\ x_{disp} \qquad D_{disp} = (\ \beta \Delta P / P_o t_{bp}\ )\ \theta_a\ x_{bp}\ x_{disp} \qquad [15]$$

Where D_{total} is the total dispersion/diffusion coefficient (m^2/day), D_{disp} is the dispersion coefficient through barometric pumping (m^2/day), D_{diff} is the effective molecular diffusion coefficient (m^2/day), A_l is the longitudinal air dispersivity (m), β is the dispersivity/travel distance ratio (dimensionless), ΔP is the pressure fluctuation range (Pa), P_o is the mean air pressure (Pa), t_{bp} is the period for pressure fluctuations (day), θ_a is the average air-filled porosity (dimensionless), x_{bp} is the depth of the barometric pressure propagation (m) and x_{disp} is the vertical travel distance (m).

Parker (2003), citing work by Gelhar et al. (1985), indicates that β generally ranges from 0.002 to 0.1 for vertical unsaturated zone transport. The ratio ΔP/Po will depend on the magnitude of the barometric pressure change and typically is less than 0.03 (Massmann and Farrier, 1992). The time period for barometric pressure fluctuations are storm dependent but often will be several days in duration. Based on the above, a reasonable range for $\beta\Delta P/P_o t_{bp}$ is taken to be $1x10^{-5}$ to $5x10^{-4}$ day^{-1}. The depth of the barometric pressure propagation will be the lesser of the depth to the capillary fringe or a depth limited by the air permeability. A conservative assumption (i.e., one that will tend to over predict the dispersion coefficient) is to assume that x_{bp} and x_{disp} are the distance from ground surface to the water table.

The relative magnitude of the dispersion coefficient to molecular diffusion coefficient was evaluated for a loam and sand soil for the range of $\beta\Delta P/P_o t_{bp}$ given above. The ratio of D_{disp}/D_{diff} shown in Figure 12 indicates that the dispersion component approaches the diffusive component for the upper range $\beta\Delta P/P_o t_{bp}$ value and deeper depths.

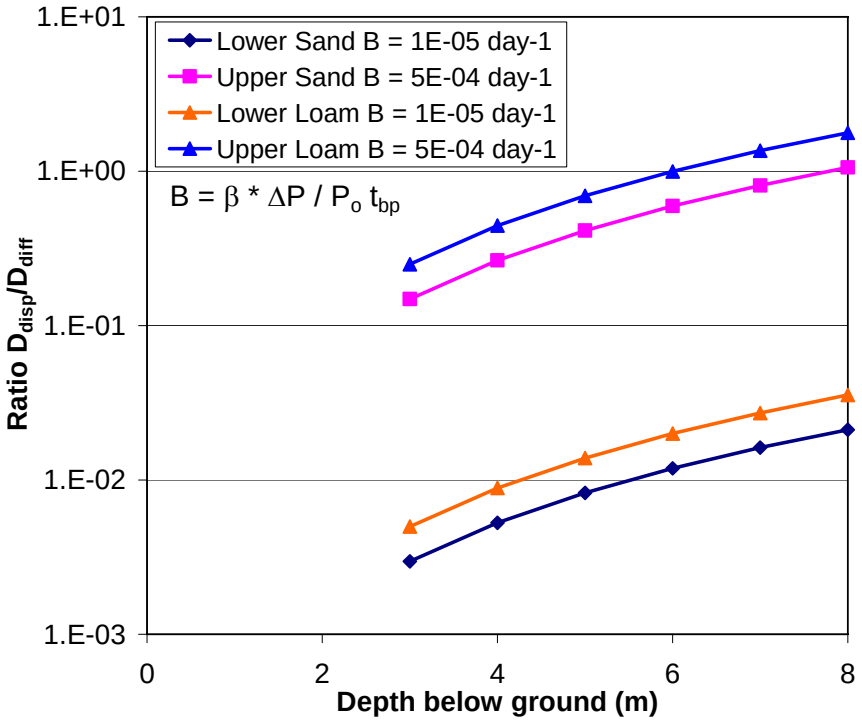

Figure 12. Relative magnitude of dispersion coefficient to molecular diffusion coefficient

Close to a building, barometric pumping may result in the movement of atmospheric air in and out of foundation subsoils. If there is a low permeability surface seal adjacent to buildings, cross-foundation slab pressure gradients may be generated when the barometric pressure decreases. One study reported measured transient cross-slab differential pressures of up to 500 Pascals (Adomait and Fugler, 1997).

In summary, barometric pressure changes may result in increased transport of hydrocarbon vapors relative to mass flux through diffusion alone; however, the same process will also result in enhanced oxygen transport to below the building. The net effect is that barometric pumping is unlikely to cause worse conditions for bioattenuation.

7.0 CASE STUDIES

Case studies are presented for sites with model input parameters for each site provided in Table 4.

7.1 Case Study One: Mount Holly, New Jersey

7.1.1 Site Description

Gasoline contamination migrated below single family houses in Mount Holly, New Jersey. Shallow soil deposits consist primarily of fine sand, that contains trace clay and silt below 7 feet depth. The depth to the water table ranged from 6.7 to 7.6 feet below ground surface near the house that was the focus of this investigation. Residual NAPL was present below 9.5 feet depth, and was submerged below the water table at the time soil vapor and indoor air testing was performed. The depth to the basement foundation was 4.5 feet.

The maximum total BTEX concentrations in shallow groundwater adjacent to the house were as high as approximately 10 mg/L; however, there were lateral concentration gradients in groundwater resulting in spatially variable and likely lower concentrations below the house. Relatively low indoor air concentrations were measured for the BTEX chemicals and other potential chemicals of interest (*e.g.,* cyclohexane). The maximum benzene, toluene, ethylbenzene, xylenes and cyclohexane concentrations measured in indoor air were 2.3 $\mu g/m^3$, 74 $\mu g/m^3$, 1.7 $\mu g/m^3$, 11 $\mu g/m^3$ and 0.34 $\mu g/m^3$, respectively. Depending on the chemical, the ratio of the subslab vapor to indoor concentrations ranged from 1.1 to 55, whereas the ratio of the external soil vapor, measured within 1 ft of the water table, to indoor air concentrations ranged from 2.1 to 200. The soil vapor monitoring results are representative of a weak vapor source.

7.1.2 Model Parameters

The modeling simulated xylene transport through a variably-saturated capillary fringe with the water-filled porosity estimated using water retention characteristics for a SCS Loamy Sand soil texture, and a first-order decay within a 0.15 m thick soil layer. Xylene was chosen since soil vapor concentrations were highest for this parameter. The building parameters were assumed to equivalent to those assumed for the development of the NJ Ground Water Screening Levels (GWSLs) (NJDEP, 2005).

7.1.3 Model Results

A first-order decay rate of 0.036 hr^{-1} provided a reasonable match between the measured and model-predicted xylenes vapor concentration profile (Figure 13). This first-order decay rate is within the range of published values for BTEX compounds presented in this paper. There were no oxygen limitations based on diffusive oxygen flux to below the building foundation, which is consistent with the near atmospheric oxygen levels measured below the slab.

The predicted vapor attenuation factor for the simulation that included first-order biodecay was $2.8x10^{-7}$, compared to $7.2x10^{-5}$ without bioattenuation. An accurate empirical attenuation factor could not be estimated since indoor xylenes concentrations are attributed to background sources. However, for comparison purposes, an "upper bound" factor ($2.7x10^{-6}$) was calculated using the measured indoor xylenes concentration. The vapor attenuation factor will be less than the upper bound factor.

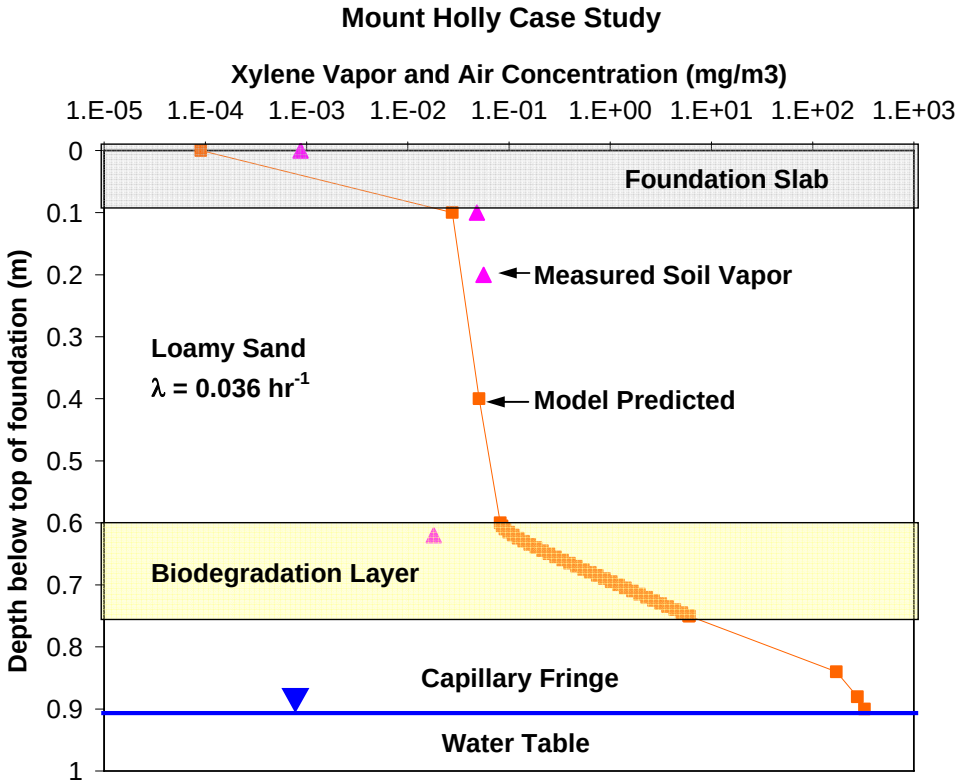

Figure 13. Model simulations for Mount Holly case study

This study highlights the influence a capillary fringe and biodegradation has on reducing vapor concentrations when there is a dissolved hydrocarbon source.

Sep-06 023-6124C

Table 4. Johnson and Ettinger Model Input Parameters for Case Studies

Location			Stafford	Stafford	Mount Holly	Paulsboro	Alameda
Scenario			Benzene	224-TMP	Xylenes	Benzene	Benzene
Chemical Properties							
	Symbol	Unit	Value	Value	Value	Value	Value
Contamination Scenario			NAPL	Dissolved	Dissolved	Likely NAPL	NAPL
Parameter (from chemical sheet)			Benzene	224 TMP	Xylene	Benzene	Benzene
Henry's Law Constant	H'	unitless	2.28E-01	1.24E+02	1.58E-01	2.28E-01	2.28E-01
Free-air Diffusion Coefficient	Dair	cm2/sec	8.80E-02	6.00E-02	7.80E-02	8.80E-02	8.80E-02
Free-water Diffusion Coefficient	Dwater	cm2/sec	9.80E-06	6.59E-06	8.70E-06	9.80E-06	9.80E-06
Soil Type, Layer Thickness and Biodegradation Rate							
Distance foundation to groundwater or vapor	Dg	m	1.50E+00	1.5	0.8	1.5	0.7
Soil Type			Sand	Sand	Loamy Sand	Loamy Sand	Sand
First-order biodegradation rate	λ_w^1	1/hr	1.0	1.0	0.036	0.0025 - 0.18	1.0
Biodegradation layer thickness	B	m	0.5	0.5	0.15	1.62	0.3
Distance top biodegradation layer from ground		m	1.65	1.65	0.5	1.68	0.55
Layer Thickness, Porosity and Water Content Parameters							
Layer 1 - Thickness	L1	m	0.230	0.230	0.020	0.324	0.050
Layer 1 - Total Porosity	θ	-	0.378	0.378	0.390	0.390	0.340
Layer 1 - Water-filled Porosity	θw	-	0.045	0.045	0.389	0.100	0.180
Layer 2 - Thickness	L2	m	0.230	0.230	0.040	0.324	0.001
Layer 2 - Total Porosity	θ	-	0.378	0.378	0.390	0.390	0.367
Layer 2 - Water-filled Porosity	θw	-	0.045	0.045	0.381	0.100	0.164
Layer 3 - Thickness	L3	m	0.230	0.230	0.090	0.324	0.001
Layer 3 - Total Porosity	θ	-	0.378	0.378	0.390	0.390	0.367
Layer 3 - Water-filled Porosity	θw	-	0.045	0.045	0.352	0.100	0.164
Layer 4 - Thickness	L4	m	0.130	0.130	0.000	0.324	0.001
Layer 4 - Total Porosity	θ	-	0.378	0.378	0.390	0.390	0.367
Layer 4 - Water-filled Porosity	θw	-	0.045	0.045	0.299	0.100	0.164
Layer 5 - Thickness	L5	m	0.330	0.330	0.000	0.324	0.001
Layer 5 - Total Porosity	θ	-	0.378	0.378	0.390	0.390	0.367
Layer 5 - Water-filled Porosity	θw	-	0.028	0.299	0.299	0.100	0.164
Layer 6 - Thickness	L6	m	0.500	0.500	0.150	1.580	0.300
Layer 6 - Total Porosity	θ	-	0.378	0.378	0.390	0.390	0.367
Layer 6 - Water-filled Porosity	θw	-	0.028	0.028	0.299	0.100	0.164
Layer 7 - Thickness	L7	m	0.001	0.001	0.200	0.001	0.001
Layer 7 - Total Porosity	θ	-	0.378	0.378	0.390	0.390	0.370
Layer 8 - Thickness	L8	m	0.001	0.001	0.300	0.390	0.370
Layer 8 - Total Porosity	θ	-	0.378	0.378	0.390	0.100	0.130
Layer 8 - Water-filled Porosity	θw	-	0.028	0.028	0.211	0.100	0.150
Layer 9 - Thickness	L9	m	0.100	0.100	0.100	0.390	0.370
Layer 9 - Total Porosity	θ	-	0.378	0.378	0.390	0.000	0.130
Layer 9 - Water-filled Porosity	θw	-	0.028	0.028	0.198	0.000	0.000
Building Properties							
Building width	W	m	4.21	4.21	10	6.24	6.0
Building length	L	m	8.67	8.67	10	6.24	8.34
Building footprint area	A	m2	36.5	36.5	100	39	50.0
Building height	H	m	2.13	2.13	3.66	2.74	2.4
Depth to base foundation below grade	D	m	1.65	1.65	2	1.68	0.2
Subsurface foundation area for vapour intrusion	Ab	m2	79.0	79.0	180	81.0	55.8
Crack width (perimeter crack)	C	mm	10	10	1	1	1
Crack ratio (perimeter Crack)	h	unitless	0.0033	0.0033	0.00022	0.00031	0.00051
Foundation thickness	T	m	0.1	0.1	0.1	0.1	0.15
Building air change rate	ACH	1/hr	0.47	0.47	0.25	0.42	1.5
Building ventilation rate	Qbuild	m3/min	0.61	0.61	1.53	0.75	3.0
Soil gas advection rate	Qsoil	L/min	2	2	5	2.8	1.35
Soil sas advection rate/building ventilation	Qsoil/Qbuild	unitless	0.0033	0.0033	0.0033	0.0037	0.00045
Effective Diffusion Coefficients							
Effective Diffusion Coefficient Layer 1	Dteff	m2/sec	1.58E-06	1.07E-06	1.55E-09	9.34E-07	1.69E-07
Effective Diffusion Coefficient Layer 2	Dteff	m2/sec	1.58E-06	1.07E-06	1.46E-09	9.34E-07	3.22E-07
Effective Diffusion Coefficient Layer 3	Dteff	m2/sec	1.58E-06	1.07E-06	2.08E-09	9.34E-07	3.22E-07
Effective Diffusion Coefficient Layer 4	Dteff	m2/sec	1.58E-06	1.07E-06	1.83E-08	9.34E-07	3.22E-07
Effective Diffusion Coefficient Layer 5	Dteff	m2/sec	1.86E-06	1.27E-06	1.83E-08	9.34E-07	3.22E-07
Effective Diffusion Coefficient Layer 6	Dteff	m2/sec	1.86E-06	1.27E-06	1.83E-08	9.34E-07	3.22E-07
Effective Diffusion Coefficient Layer 7	Dteff	m2/sec	1.86E-06	1.27E-06	8.11E-08	9.34E-07	5.52E-07
Effective Diffusion Coefficient Layer 8	Dteff	m2/sec	1.86E-06	1.27E-06	1.66E-07	9.34E-07	5.52E-07
Effective Diffusion Coefficient Layer 9	DTeff	m2/sec	1.86E-06	1.27E-06	2.10E-07	2.51E-06	5.52E-07

7.2 Case Study Two: Paulsboro, New Jersey

7.2.1 Site Description

Gasoline contamination migrated below single family houses in Paulsboro, New Jersey. Shallow soil deposits consist primarily of fine to medium sand, with small fractions of silt and coarse sand. The depth to groundwater is approximately 18 feet below ground surface. Residual NAPL is inferred to be present at the water table. The depth to the basement foundation was approximately 5.5 feet.

Soil vapor concentrations were measured below a house at 8, 12 and 16 feet depth below ground surface, and at the same depths external to the house. While similar BTEX concentrations were measured in the deepest soil vapor sample, at 8 feet depth (approximately 2.5 feet below the foundation) the BTEX concentrations below the house were about two orders-of magnitude higher than beside the house. The oxygen concentrations below the house at 8 feet were about 1 percent, while beside the house at the same elevation were 14.5 percent. The average total BTEX concentrations below the house at 8, 12 and 16 feet depth were 2,559, 1,818 and 3,070 mg/m^3, respectively. The total BTEX concentration in indoor air was 30 $\mu g/m^3$.

7.2.2 Model Parameters

The modeling simulated BTEX transport through unsaturated soil with constant water-filled porosity estimated using water retention characteristics for a SCS Loamy Sand soil texture. The water-filled porosity was assumed to be equal to the field capacity for Loamy Sand (θ_w = 0.10). The input parameters for building properties consisted of a combination of site specific and assumed values.

First-order biodecay was assumed to occur within a 5.3 ft. thick layer directly below the building. This thickness is equal to 1/3 the vadose zone thickness. Oxygen transport to below the slab was assumed to be limited to diffusion. The physical dimensions for oxygen transport were similar to those assumed for the model scenarios in Table 2. The stoichiometric ratio (SR) for oxygen to hydrocarbon demand ratio was taken to be three. The maximum hydrocarbon flux (F_o) aerobically degraded is calculated to be 4.1 mg/s. The oxygen demand for methane oxidation was not considered. An initial first-order decay rate of 0.18 hr^{-1} was assumed.

Since gasoline comprises many other hydrocarbon compounds beyond BTEX, the maximum BTEX flux aerobically degraded was scaled downward to reflect the oxygen demand other hydrocarbon compounds will have. An approximate scaling ratio was estimated considering the following:

- The theoretical ratio of the predicted BTEX to total hydrocarbon vapor concentration calculated from Raoult's Law (i.e., mole fraction multiplied by vapor pressure), based on data presented in Johnson et al. (1990), ranges from 0.0075 (fresh gasoline) to 0.074 (weathered gasoline);

- USEPA (1995) present BTEX and total hydrocarbon (TPH) soil vapor concentrations measured at a number of bioventing sites. For gasoline contamination, the ratio of the BTEX to TPH concentrations generally ranged from 0.01 to 0.04; and

- Parker (2003) for modeling of bioattenuation at the Paulsboro site estimated that the BTEX decay accounts for less than 2% of the total oxygen demand.

Based on the above, a scaling ratio of between 0.01 and 0.04 was adopted for the model simulations.

7.2.3 Model Results

The model results indicate that the estimated scaling ratio for the BTEX to total TPH oxygen demand has an effect on model predictions (Figure 14). For a scaling ratio of 0.01, there were oxygen limitations in that the first-order decay rate had to be reduced to 0.0025 hr^{-1} so that the oxygen demand did not exceed supply, whereas for a scaling ratio of 0.04, there were no oxygen limitations. The predicted vapor attenuation ratios for the two scenarios were $7.6x10^{-4}$ (scaling ratio of 0.01) and $3.7x10^{-7}$ (scaling ratio of 0.04). The upper bound empirical attenuation factor was approximately $1x10^{-5}$.

.

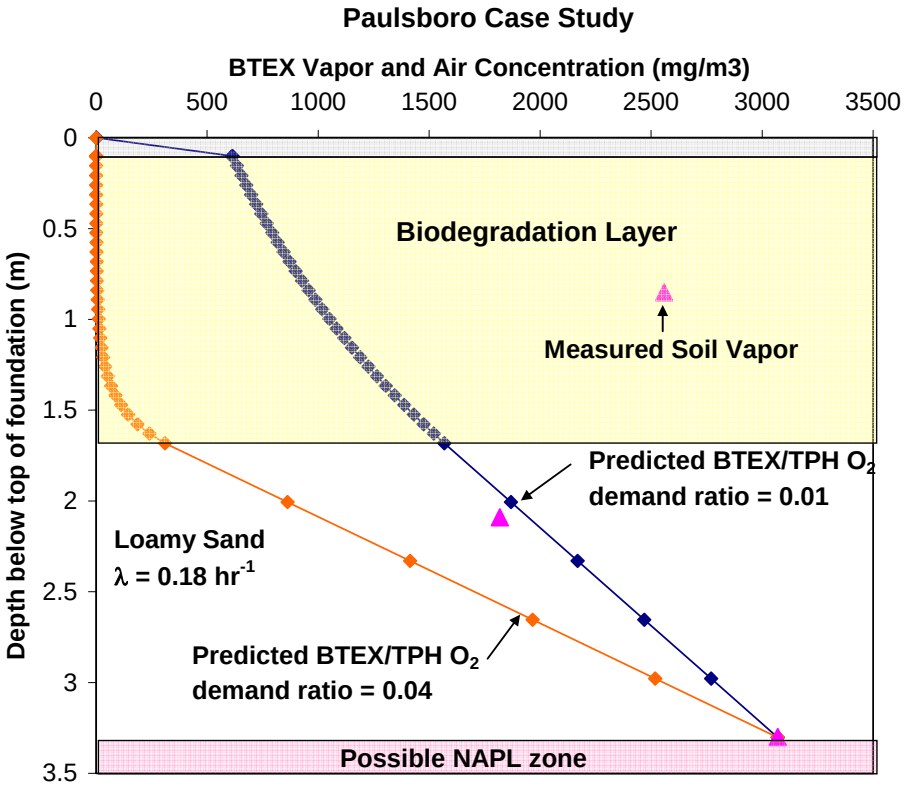

Figure 14. Model simulations for Paulsboro case study

The results indicate the sensitivity of the model predictions to calculations of oxygen availability, but suggest oxygen limitations below the building at the Paulsboro site may be plausible. Other sensitive parameters include the soil water-filled porosity and the biodegradation layer thickness. The model simulations should not be viewed deterministically but one of many possible model realizations.

7.3 Case Study Three: Stafford Township, New Jersey

7.3.1 Site Description

This case study, described in Sanders and Hers (2006), is a site where gasoline contamination migrated below single family houses in Stafford Township, New Jersey. Shallow soil consists of fine to medium sand. The depth to the water table was 10.8 feet below ground surface. Residual NAPL is inferred to be present at the water table. The depth to the basement foundation was approximately 5.5 feet.
\
Concentrations of volatile organic chemicals in the groundwater were as high as 82 mg/L for total BTEX and up to 590 mg/L for methyl-t-butyl ether (MTBE). The maximum deep soil vapor concentrations within 6 feet laterally from the house and 1 to 2 feet of the water table were 656 mg/m^3 for benzene, 1,920 mg/m^3 for 2,2,4-trimethylpentane (TMP) and 1,060 mg/m^3 for cyclohexane. For a house situated above the NAPL zone, there were elevated 2,2,4-TMP and cyclohexane concentrations in subslab soil vapor and indoor air; however, BTEX concentrations in indoor air were low and near background levels. The vapor concentrations at the opposite side of the house were at low μg/m^3 levels.

	Vapor and Indoor Air Concentrations (mg/m^3)			
Location	Benzene	2,2,4-Trimethylpentane	Cyclohexane	Total Hydrocarbon
Deep Soil Vapor	656	1,920	1,060	75,000
Deep Soil Vapor Used for Modeling	328	960	N/A	N/A
Subslab Vapor	<0.984	96	15	N/A
Basement	<0.0016	0.70	0.13	N/A

7.3.2 Model Parameters

The modeling simulated benzene and 2,2,4-TMP transport through unsaturated soil with water-filled and total porosity estimated from soil water retention testing and gravimetric moisture content analysis. The unsaturated soil below the foundation was divided into two 0.84 m thick layers; in the top layer, the water-filled porosity was a value half-way between the field capacity and residual saturation (0.028), while in the bottom layer, the water-filled porosity was the field capacity (0.045). The total-porosity was 0.378. The input parameters for building properties consisted of a combination of site specific and assumed values.

First-order biodecay was assumed to occur within a soil layer that was one-third (1.1 m) the thickness of the unsaturated zone (3.3 m). Since the depth to the base of the foundation was 1.7 m, the thickness of the biodegradation layer below the building was 0.5 m. Oxygen transport to below the slab was assumed to be limited to diffusion. The physical dimensions for oxygen transport were similar to those assumed for the model scenarios in Table 2. The stoichiometric ratio (SR) for oxygen to hydrocarbon demand ratio was taken to be three. The maximum hydrocarbon flux (F_o) aerobically degraded is calculated to be 4.3 mg/s. To account for oxygen demand by other hydrocarbon constituents in gasoline vapors, the maximum hydrocarbon flux was scaled by the ratio of the individual hydrocarbon to total hydrocarbon concentration; therefore, for benzene F_o was equal to 0.38 mg/s (4.3 mg/s*656/75,000). The oxygen demand for methane oxidation was not considered.

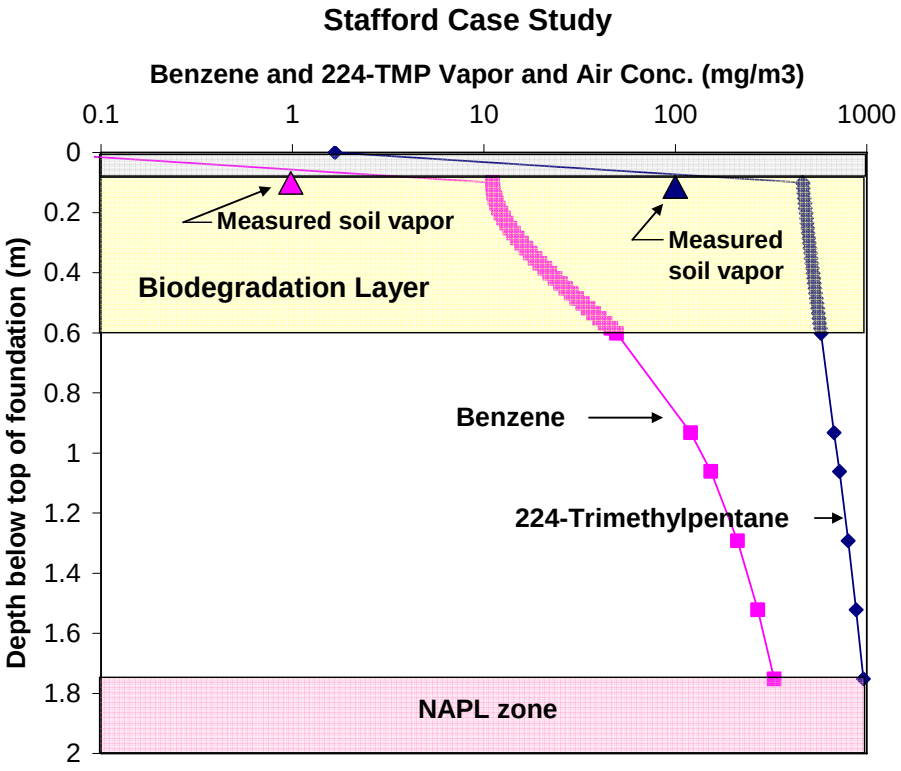

Figure 15. Model simulations for Stafford case study

7.3.3 Model Results

For the Stafford case study a different approach was taken for determination of the first-order decay rate. Since initial modeling conducted using mid-range decay constants indicated little hydrocarbon degradation was predicted directly below the foundation, the decay constant was increased until either a reasonable upper bound decay rate or oxygen limitations were reached. The model simulations indicated that no oxygen limitations

were identified for the upper bound rates, which were taken to be 1 hr^{-1} for benzene and 10 hr^{-1} for 2,2,4-TMP based on information provided in Table 1.

The predicted soil vapor profiles for the upper bound decay constants indicate that the predicted vapor concentrations below the foundation slab were approximately one order-of-magnitude greater than the measured vapor concentrations (Figure 15). The predictions are to a degree consistent with field observations in that greater attenuation was predicted for benzene than 2,2,4-TMP. A closer match between predicted and measured vapor concentrations would have been obtained for a thicker biodegradation layer and higher soil moisture contents.

It is hypothesized that while there are likely no oxygen limitations below the building foundation[1], due to the shallow contamination, high source concentrations and low soil moisture (which results in a high hydrocarbon vapor flux), there is insufficient transport distance and time for complete degradation of hydrocarbon vapors (i.e., kinetics are not fast enough). It is noted that although the 2,2,4-TMP concentrations were elevated below the building foundation, significant attenuation nevertheless occurred within the vadose zone (about one-of-magnitude). Greater attenuation was observed for benzene even though first-order decay rates for benzene were lower than for 2,2,4-TMP. This is because of the higher sources strength for 2,2,4-TMP. These findings, although preliminary, may be important when interpreting oxygen data for other sites.

7.4 Case Study Four: Alameda, California

7.4.1 Model Parameters

Gasoline contamination migrated below a commercial building at the Alameda Air Force site in San Francisco Bay area of California (Fischer et al., 1996). The building has a footprint area of 50 m^2, a slab-at-grade foundation, and is underlain by fill soils comprised of sand. The depth to the contamination source (inferred to be residual NAPL) is approximately 1.5 m below ground surface. A vertical profile indicated a sharp decrease in hydrocarbon vapor concentrations between 0.7 m and 0.4 m depth below ground surface, and a corresponding increase in oxygen concentrations. The iso-pentane and benzene concentrations in soil vapor at 0.7 m depth were 28,000 mg/m^3 and 200 mg/m^3, respectively.

7.4.2 Model Parameters

The modeling simulated iso-pentane and benzene transport through unsaturated soil. The soil and building parameters were based on values provided by Fischer et al. (1996). The thickness of the first-order biodecay layer (0.3 m) was estimated from the vertical profile of hydrocarbon and oxygen concentrations below the foundation. Similar assumptions for oxygen transport were assumed as for other case studies. The maximum hydrocarbon flux (F_o) aerobically degraded is 3.3 mg/s. To account for oxygen demand by other

[1] No oxygen measurements were obtained below the slab due to equipment malfunction.

hydrocarbon constituents in gasoline vapors, the maximum hydrocarbon flux was scaled by the ratio of the vapor concentration to total hydrocarbon vapor concentration, predicted from Raoult's Law for a weather gasoline (Johnson et al., 1990). For iso-pentane, a scaling ratio of 0.03 was used, resulting in a maximum F_o for iso-pentane of 0.1 mg/s. For benzene, a scaling ratio of 0.01 was used.

7.4.3 Model Results

A similar approach was taken for determination of the decay constant as for the Stafford case study. For iso-pentane, the first-order decay constant was adjusted until the oxygen consumption met the oxygen supply, resulting in a first-order decay constant of 0.4 hr^{-1}. For benzene, there were no oxygen limitations identified for a first-order decay constant of 1 hr^{-1} (upper rate); however, predictions are less meaningful since oxygen is likely limited due to demand by iso-pentane and other volatile components.

The predicted iso-pentane concentration soil vapor profile indicates limited bioattenuation and higher predicted than measured vapor concentrations (Figure 16). The divergence between the measured and predicted rates is unknown but may be related to the smaller building size and slab-at-grade construction, and possibly other mechanisms for oxygen migration to below foundation such as barometric pumping. In addition, since the soil vapor profile was obtained approximately 1.5 m from the edge of the foundation, there may have been higher hydrocarbon vapor concentrations below the middle of the slab.

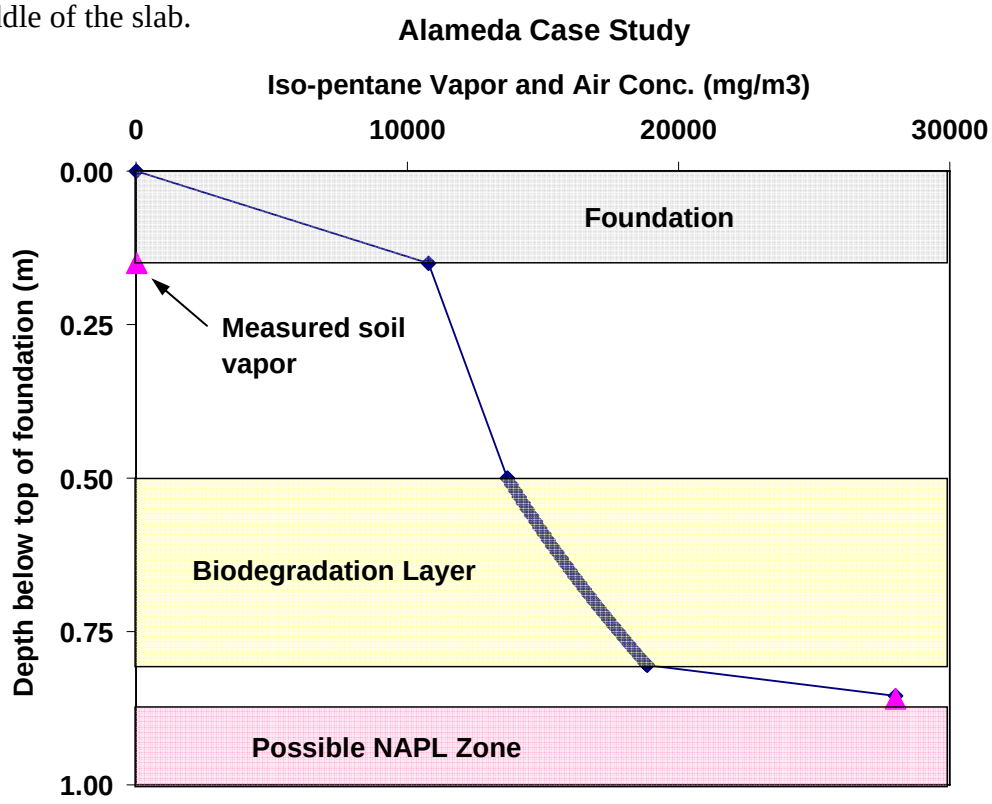

Figure 16. Model simulations for Alameda case study

8.0 REGULATORY IMPLICATIONS

The regulatory implications of model simulations presented in this paper are discussed in the context of possible adjustments to generic or semi-site specific attenuation factors. The models presented in this paper are also considered appropriate for site-specific assessment of bioattenuation when there is evidence of biodegradation and sufficient data.

8.1 Key Factors Identified through Modeling

The modified J&E model incorporating oxygen-limited first-order decay predicts a range of attenuation factors depending on the input parameters. For some scenarios, there are order-of-magnitude differences between the factors for the degrading and non-degrading cases. The model-predicted attenuation factors vary strongly as a function of source concentrations, soil moisture and separation distance between the foundation and source.

For dissolved plumes, the model predictions indicate that the presence of the capillary fringe significantly reduces volatilization flux due to higher soil moisture near the water table. While there may be short term increases in volatilization flux due to a decrease in the water table, on a longer-term basis, there will likely be sufficient re-oxygenation in the vadose zone for hydrocarbon degradation at most sites above dissolved phase plumes.

The major process for oxygen transport to below building foundations is likely diffusion, although wind-induced movement and barometric pumping of soil gas may also contribute to oxygenation under certain site conditions. Surface barriers may or may not be important depending on the construction, porosity, and cracks and openings for oxygen diffusion. The model simulations in this paper assume no oxygen transport through the building foundation, which is conservative. A preliminary assessment of building size indicates that bioattenuation decreases with increasing building size, assuming no oxygen migration through the foundation.

8.2 Site Characterization

A sufficiently detailed site investigation should be completed and conceptual site model (CSM) developed prior to the vapor intrusion assessment. In particular, NAPL source zones should be well characterized. There are many investigation methods and tools that can be used to build the CSM including continuous soil cores, field indicator tests such vapor headspace measurements and shake tests, vertical profiling of media concentrations (soil, groundwater, soil vapor), and sensors (MIP, UVIF) that be used with direct-push technologies to infer contamination zones. Vertical profiles and lateral transects of soil vapor concentrations can be very useful in developing the CSM and corroborating data quality. Possible future changes in site conditions should be taken into consideration when evaluating the CSM including a possible decline in water table that would expose NAPL zones to soil gas.

8.3 Groundwater Attenuation Factors

Where contamination is limited to a dissolved source, the following preliminary bioattenuation reduction factors are recommended for adjustment of currently employed generic groundwater attenuation factors (i.e., 10^{-3}) for BTEX compounds:

Gasoline (TPH_g > 50 ppm): 10X for separation distance > 1 m

Diesel (TPH_d < 10 ppm): 100X for separation distance > 1 m

A higher reduction factor for diesel is warranted due to lower compound solubility and hence significantly lower source strength.

It is generally recommended that soil vapor measurements be made to confirm predictions from groundwater since there is uncertainty in delineation of NAPL boundaries and predictive models for transport within the capillary fringe. In addition, since dissolved plumes tend to be relatively short, as a practical consequence, there may be limited ability to screen out sites based on groundwater data alone.

8.4 Soil Vapor Attenuation Factors

Soil vapor measurements should be made whenever there are NAPL source zones or soil contamination above the water table. For a soil vapor contamination source within the unsaturated zone, hydrocarbon vapor bioattenuation is more sensitive to key factors (source concentrations, distance from building to source, soil water-filled porosity, surface capping effect) than for a dissolved groundwater source. Therefore, it is important to develop a protocol that incorporates these factors, as recommended below:

1. Adequately characterize the contamination source through a multiple lines of evidence approach described above.

2. Obtain data on deep external soil vapor concentrations (TPH, methane[2] and specific compounds of concern) near to, but above, the contamination source.

3. Obtain soil vapor profile data (hydrocarbon, oxygen, carbon dioxide) to confirm biodegradation is occurring. There should be evidence of bioattenuation occurring below the elevation of the building through a increase in hydrocarbon and carbon dioxide concentrations with increasing depth (as you approach the source), and decreasing oxygen concentrations with increasing depth (as oxygen is utilized). Ideally, profiles should be obtained below a portion of the buildings at a site, or when external to the building, should be from below a paved surface.

[2] Although oxygen-demand for biodegradation of methane was not addressed in case studies due to limited data, it is potentially important, and as discussed below, further research on potential significance of methane oxidation is needed.

4. Assess whether there is potential for significant capping effect. There is currently insufficient basis for establishing a generic criteria for whether there is a significant capping effect so professional judgment is require to assess this.

5. Using deep soil vapor data, apply model-predicted order-of-magnitude reduction factors calculated using reasonably conservative soil-water filled porosity values and first-order decay constants. The Abreu and Johnson (2006) model predictions for the mid-range first-order decay constant (0.18 hr^{-1}) are considered to provide a preliminary basis for determining such reduction factors:

Cg > 50 mg/L:	10X for separation distance > 5 m
Cg > 1 mg/L < 50 mg/L:	10X for separation distance > 2 m 100X for separation distance > 4 m
Cg < 1 mg/L:	10X for separation distance > 1 m 100X for separation distance > 3 m

   The soil gas concentration should be the measured TPH concentration including methane.

8.4.1 Further Work

Additional study is needed in a number of areas:

1. While the Johnson and Abreu (2006) simulations incorporate reasonably conservative inputs for soil moisture (sand) and building properties, further sensitivity analysis of parameters (water-filled porosity, Q_{soil}) influencing alpha would add insight beyond those factors already investigated.

2. Model simulations evaluating influence of bioattenuation on attenuation factors for commercial buildings.

3. A standardized protocol for measurement of TPH soil vapor.

4. Additional study of biodegradation kinetics for non-BTEX hydrocarbon compounds and relative oxygen demand for different hydrocarbon compounds including methane.

9.0 CONCLUSIONS

The J&E-BIO semi-analytical model is a relatively simple modeling tool that can be used to provide insight on influence of bioattenuation on vapor transport below buildings and vapor intrusion. The J&E-BIO model, which incorporates oxygen-limited biodecay, was benchmarked against the 3-D numerical model by Abreu and Johnson, and was found to predict similar attenuation factors. The J&E-BIO model was used to evaluate several

different scenarios relative to the base case simulations, which were for a homogeneous soil profile. The model simulations are approximate.

The key findings were the higher soil moisture as found within the capillary fringe significantly reduces volatilisation flux of hydrocarbons. As a consequence, the model simulations suggest oxygen limitations below buildings above dissolved hydrocarbon sources would be rare, except when contamination was very shallow. The model simulations suggest the influence of wind on oxygenation below buildings will typically be relatively minor. Barometric pressure changes may result in increased transport of hydrocarbon vapors relative to mass flux through diffusion alone; however, the same process should also result in enhanced oxygen transport to below the building. The modeling suggests competent low permeability or diffusivity surface barriers may significantly reduce oxygenation below buildings.

The case studies each reveal different modeling behaviors. For Mount Holly, biodegradation reduced vapor concentrations to negligible levels due to the small mass flux through the capillary fringe. For Paulsboro, a site with NAPL above the water table, depending on the assumptions for oxygen transport and relative oxygen demand for hydrocarbon compounds, there were significant differences in bioattenuation and oxygen limitations. For Stafford, the measured hydrocarbon vapor concentrations below the building were elevated despite model predictions that suggested no oxygen limitations. It is speculated that this may be due to kinetic limitations resulting in incomplete decay below the slab due to high source concentrations, dry soils and a small transport distance. For Alameda, oxygen limitations were predicted using a diffusion model, and higher predicted than measured vapor concentrations were obtained suggesting the possibility of additional mechanisms for oxygen transport to below the foundation.

GOLDER ASSOCIATES LTD.

ORIGINAL SIGNED BY

Todd H. Rees, Ph.D., P.E.
Principal

ORIGINAL SIGNED BY

Ian Hers, Ph.D., P.Eng.
Associate, Senior Environmental Engineer

TH/IH/jc
023-6124-001
N:\Final\2002\6000\023-6124C\Influence of Bioattenuation\rep 0911 Bio Modeling.doc

10.0 REFERENCES

Abreu, L. and P.C. Johnson. 2005. Effect of Vapor Source-Building Separation and Building Construction on Soil Vapor Intrusion as Studied with a Three-Dimensional Numerical Model. *Environ. Sci. Technol*. 2005, **39**, 4550-4561

Abreu, L. and P.C. Johnson. 2006. Simulating the Effect of Aerobic Biodegradation on Soil Vapor Intrusion into Buildings: Influence of Degradation Rate, Source Concentration, and Depth. *Environ. Sci. Technol*. 2006, **40**, 2304-2315

Adomait, M., D. Fugler. A Method to Evaluate Soil Gas VOC Influx into Houses. In *Proc. of Air and Waste Management Association's 90th Annual Meeting and Exhibition*, June 8-13, 1997, Toronto, Ontario, Canada.

Culot, M.J.V., Olson, H.G., Schiager, K.J. 1976. Effective diffusion of radon in concrete: theory and method for field measurements. *Health Physics*. **30**: 263-270.

Davis, G.B., T.R. Power, D. Briegel and B.M.Patterson. BTEX vapour biodegradation rates in vadose zone: initial estimates. *Groundwater Quality: Remediation and Protection. Proc. Of the GQ'98 Conference*, Tubingen, Germany, September 1998. IAHS Publ No. 250, 1998.

DeVaull, G., R. Ettinger, J. Gustafson. 2002. Chemical Vapor Intrusion from Soil or Groundwater to Indoor Air: Significance of Unsaturated Zone Biodegradation of Aromatic Hydrocarbons, *Soil and Sediment Contamination*, Vol. **11**, No. 4, pp. 625-641.

DeVaull, G., R.A. Ettinger, J.P. Salanitro, and J. Gustafson., 1997. Benzene, toluene, ethylbenzene and xylenes degradation in vadose zone soils during vapor transport: first-order rate constants. Proceedings of 1997 Petroleum Hydrocarbons and Organic Chemicals in Ground Water, *API/NGWA*, Houston, Texas, November, 365-379.

Fischer, M.L., A.J. Bentley, K.A. Dunkin, A.T. Hodgson, W.W. Nazaroff, R.G. Sextro, and J.M. Daisey. 1996. Factors Affecting Indoor Air Concentrations of Volatile Organic Compounds at a Site of Subsurface Gasoline Contamination. *Environ. Sci. Technol.* **30** (10): 2948-2957.

Folkerts, K.H. et al. (1984) "An experimental study on diffusion and exhalation of 222Rn and 220Rn from building materials", *Radiation Protection Dosimetry*, **9**(1), 27-34.

Gaganis, P., P.K. Kjelsen, V.N. Burganos. 2003. Cost-effective modeling of fuel mixture transport in the vadose zone: Application to a field experiment, Airbase Vaerlose, Denmark. 2nd Int. Work Shop on *Groundwater Risk Assessment at Contaminated Sites and Integrated Soil and Water Protection, Tubingen. Tubingen. Tubinger Geowissenschaftliche Arbeiten* Vol. **69**. pp. 53-58.

Gelhar, L., T-CJ Yeh and A.L. Gutjahr. 1985. Stochastic Analysis of Unsaturated Flow in Heterogeneous Soils; 3. Observations and Applications. *Water Resources Research* Vol. **21**, No. 4, p 465-471, April, 1985

Golder Associates Ltd. 2004. Soil Vapor Intrusion Guidance for Health Canada Screening Level Risk Assessment (SLRA), November 9.

Hers, I., H. Dawson and R. Truesdale. 2006. Status of Generic Screening Levels – Update on Empirical Vapor Attenuation Factor Analysis. *Presentation at workshop held at 16th Annual AEHS Meeting & West Coast Conference on Soils, Sediments and Water,* March 15th – 19th, 2006, San Diego, California.

Hers, I., R. Zapf-Gilje, P.C. Johnson, and L. Li. 2003d. Evaluation of the Johnson and Ettinger model for prediction of indoor air quality. *Ground Water Monitoring and Remediation*, Summer 2003.

Hers, I., J. Atwater, L. Li, and R. Zapf-Gilje. 2000a. Evaluation of vadose zone biodegradation of BTX vapours. *Journal of Contaminant Hydrology*, **46**, 233-264.

Hohener, P., C. Duwig, G. Pasteris, K. Kaufmann, N. Dakhel, H. Harms, J. 2003. Biodegradation of petroleum hydrocarbon vapors: laboratory studies on rates and kinetics in unsaturated alluvial sand. *J. of Contam. Hydrol*., **66**, pp. 93-115.

Jin, Y.T, Streck, T., Jury, W.A. 1994. Transport and biodegradation of toluene in unsaturated zone soil. *J. of Contaminant Hydrology*, **17**, 111-127,

Johnson, P.C. 2006. Field Studies of Oxygen and Hydrocarbon Vapor Transport Beneath and Around Buildings Located over NAPL Sources. Presentation at *USEPA/AEHS Work Shop on USEPA Vapor Intrusion Guidance Revisions*, San Diego, March 16.

Johnson, P.C. 2002. Migration of Soil Gas Vapours to Indoor Air. Determining Vapor Attenuation Factors Using Screening-Level Model and Field Data from *the CDOT MTL, API Bulletin* 16, April.

Johnson, P. C., M. W. Kemblowski, and R. L. Johnson. 1999. Assessing the Significance of Subsurface Contaminant Vapor Migration to Enclosed Spaces: Site-Specific Alternatives to Generic Estimates. *Journal of Soil Contamination*, **8**, 389-421.

Johnson, P.C., W. Kemblowski, and R.L. Johnson. 1998. Assessing the Significance of Subsurface Contaminant Vapor Migration to Enclosed Spaces – site specific alternatives to generic estimates. *API Publication.*

Johnson, P.C. and R. Ettinger. 1991. Heuristic Model for Predicting the Intrusion Rate of Contaminant Vapours into Buildings. *Environ. Sci. Technol.* **25** (8):1445-1452.

Johnson, P.C., M.W. Kemblowski and J.D. Colthart. 1990 Quantitative analysis for the cleanup of hydrocarbon-contaminated soils by in-situ venting. *Groundwater*. **28**(3):413-29.

Lahvis, M.A. and A.L. Baehr. 1996. Estimation of rates of aerobic hydrocarbon biodegradation by simulation of gas transport in the unsaturated zone. *Water Resources Research.* **32**(7): 2231-2249, July. CHECK THAT R-UNSAT REFERENCE

Lahvis, M.A. and A.L. Baehr. 1996. Quantification of aerobic biodegradation and volatilization rates of gasoline hydrocarbons near the water table under natural attenuation conditions. *Water Resources Research*, Vol. **35**, No.3, pp. 753-765. March.

Laubacher, R.C. P. Bartholomae, P. Velasco, and H.J. Reisinger. 1997. An evaluation of the vapor profile in the vadose zone above a gasoline plume. Proceedings of 1997 *Petroleum Hydrocarbon and Organic Chemicals in Ground Water*, Houston, Texas, November, 396-409.

Li., H., J.J. Ji and M. Luke. 2004. A falling-pressure method for measuring air permeability of asphalt in laboratory. *Journal of Hydrology*, **286**, pp. 69-77.

Maier, U., U. Mayer, P. Grathwohl. 2003. Modeling transport and natural attenuation of fuel compounds in the vadose at the emplaced fuel source experiment, Airbase Vaerlose, Denmark, 2nd International Work Shop on *Groundwater Risk Assessment at Contaminated Sites and Integrated Soil and Water Protection, Tubingen, Tubinger Geowissenschaftliche Arbeiten* Vol. **69**, pp. 47-52.

Massman, J. and D.F. Farrier. 1992. Effects of atmospheric pressures on gas transport in the vadose zone. *Water Resources Research.* **28** (3):777-791.

Millington, R.J. and J.M. Quirk. 1961. Permeability of porous solids. *Trans. Farady Soc:*, 1200-1207.

New Jersey Department of Environmental Protection (NYDEP). 2005. Vapor Intrusion Guidance.

Nielson, K.K., V.C Rogers, R.B. Holt, T.D. Pugh, W.A. Grondzik and R.J de Meijer. 1997. *Radon Penetration of Concrete Slab Crakcs, Joints, Pipe Penetrations and Sealants. Health Physics*, **73**(4): 668-678.

Olson, J.J., Mills, G.L., Herbert, B.E. and Morris, P.J. 1999. Biodegradation Rates of Separated Diesel Components. *Environmental Toxicology and Chemistry*, **18**, pp. 2448-2453.

Ostendorf, D.W. and D.H. Kampbell. 1991. Biodegradation of hydrocarbon vapours in the unsaturated zone. *Water Resources Research.* **27** (4):453-462.

Parker, J. C. 2003. Modeling Volatile Chemical Transport, Biodecay, and Emission to Indoor Air. *Ground Water Monitoring and Remediation* **23**:107-120.

Pasteris, G; D. Werner, K. Kaufmann, P. Hohener. 2002. Vapor Phase Transport and Biodegradation of Volatile Fuel Compounds in the Unsaturated Zone: A Large Scale Lysimeter Experiment. *Environ. Sci. Technol.* **36**, 30-39.

Renken, K.J. and T. Rosenberg 1995. Laboratory Measurement of the Transport of Radon Gas through Concrete Samples. *Health Physics*, **68/6**, pp. 800-808.

Ririe, T. and R. Sweeney. 1995. Fate and transport of volatile hydrocarbons in the vadose zone. Proceedings of *1995 Petroleum Hydrocarbon and Organic Chemicals in Groundwater, Houston, Texas*, 529-542.

Rogers, V.C., K.K. Nielson, R.B. Holt and R. Snoddy. Radon Diffusion Coefficients for Residential Concretes. *Health Physics*. **67**(3): pp. 261-265.

Sanders, P. and Hers, I. 2006. Vapor Intrusion in Homes over Gasoline-Contaminated Ground Water in Stafford, New Jersey. *Ground Water Monitoring and Remediation*, Winter.

Schaap M.G., Leij F.J. 1998. Database related accuracy and uncertainty of pedotransfer functions. *Soil Sci*. **163**:765-779.

Siotis, I, Wrixon, A.D. (1984) "Radiological consequences of the use of fly ash in building materials in Greece", *Radiation Protection Dosimetry*, **7**(1-4), 101-105.

Stranden E., Kolstad E., Lind B., The influence of moisture and temperature on radon exhalation, *Rad. Prot. Dos.*, **7**(1-4):55-58, 1984. [20]

USEPA 2002. Draft USEPA Vapor Intrusion Guidance, November.

USEPA, 1995. *Bioventing Principles and Practice Vol. 1: Bioventing Principles*, Washington, D.C.